

REVIEW

Open Access Prediction of the Madden–Julian Oscillation: A Review

HYEMI KIM

School of Marine and Atmospheric Sciences, Stony Brook University, Stony Brook, New York

FRÉDÉRIC VITART

European Centre for Medium-Range Weather Forecasts, Reading, United Kingdom

DUANE E. WALISER

Jet Propulsion Laboratory, California Institute of Technology, Pasadena, California

(Manuscript received 6 April 2018, in final form 1 July 2018)

ABSTRACT


There has been an accelerating interest in forecasting the weather and climate within the subseasonal time range. The Madden–Julian oscillation (MJO), an organized envelope of tropical convection, is recognized as one of the leading sources of subseasonal predictability. This review synthesizes the latest progress regarding the MJO predictability and prediction. During the past decade, the MJO prediction skill in dynamical prediction systems has exceeded the skill of empirical predictions. Such improvement has been mainly attributed to more observations and computer resources, advances in theoretical understanding, and improved numerical models aided in part by multinational efforts through field campaigns and multimodel experiments. The state-of-the-art dynamical forecasts have shown MJO prediction skill up to 5 weeks. Prediction skill can be extended by improving the ensemble generation approach tailored for MJO prediction and by averaging multiensembles or multimodels. MJO prediction skill can be influenced by the tropical mean state and low-frequency climate mode variations, as well as by the extratropical circulation. MJO prediction skill is proven to be sensitive to model physics, ocean–atmosphere coupling, and quality of initial conditions, while the impact of the model resolution seems to be marginal. Remaining challenges and recommendations on new research avenues to fully realize the predictability of the MJO are discussed.

1. Introduction

There has been a growing interest in forecasting the weather and climate within the subseasonal range (i.e., 3–4 weeks), which lies in between the medium-range weather and seasonal forecasts. The subseasonal forecast is particularly important since many management decisions, including those related to water, food, and hazard considerations, fall into this range. Skillful predictions of anomalous weather events, such as extreme precipitation events, in the subseasonal time scale could provide policy makers, emergency managers, and stakeholders with

advance notice to prepare for mitigating actions (e.g., [National Academies of Sciences, Engineering, and Medicine 2016](#)). Realizing the need for subseasonal prediction, there have been ongoing efforts at operational centers in producing subseasonal forecasts and expending these resources to application communities (e.g., energy sector) who have become convinced of the potential benefits of the subseasonal forecast regarding its social and economic value.

The Madden–Julian oscillation (MJO; [Madden and Julian 1971, 1972](#)) is recognized as one of the leading sources of subseasonal predictability (e.g., [Waliser 2011](#); [Zhang et al. 2013](#)). The MJO is an organized envelope of tropical convection with a life cycle of about 40–50 days, fitting neatly within the subseasonal time scale (30–90 days). It is characterized by a vast zonal scale (wavenumber 1–3) and a dominant eastward propagation

 Denotes content that is immediately available upon publication as open access.

Corresponding author: Hyemi Kim, hyemi.kim@stonybrook.edu

DOI: 10.1175/JCLI-D-18-0210.1

© 2018 American Meteorological Society. For information regarding reuse of this content and general copyright information, consult the [AMS Copyright Policy](#) (www.ametsoc.org/PUBSReuseLicenses).

over the tropical Indo-Pacific basin, particularly during the boreal winter season. The MJO-associated convection and circulation anomalies affect global weather and climate, acting as a primary source of subseasonal predictability for the global weather and climate system (e.g., Zhang 2005, 2013; Brunet et al. 2010; National Research Council 2010; Lau and Waliser 2011; Zhang et al. 2013; National Academies of Sciences, Engineering, and Medicine 2016). Real-time MJO forecasts are now produced routinely by many centers, a big difference since the community's first attempts at cobbling together (experimental) operational MJO forecasts (Waliser et al. 2006). For example, NOAA/CPC¹ produces a weekly update of MJO status and forecast, in addition to the dynamical model MJO forecasts every day.

Until about a decade ago, MJO prediction with empirical techniques often had higher skill than numerical models (Waliser 2006a,b). Then, several studies demonstrated that MJO prediction in some numerical models has exceeded the skill of empirical models (review by Waliser 2011; Lee et al. 2017). The improvement of MJO prediction by numerical models has been mainly attributed to advances in theoretical understanding and significant improvements of the dynamical forecasting systems—including more observations and computer resources, better data assimilation techniques, and improved numerical models (e.g., review by Kim and Maloney 2017) aided in part by multinational efforts through field campaigns and numerical model experiments (Petch et al. 2011; Moncrieff et al. 2012; Waliser et al. 2012; Yoneyama et al. 2013; Klingaman et al. 2015b). Nevertheless, estimates of the predictability of the MJO suggest that there is still considerable room for improvement.

After the in-depth holistic review by Waliser (2011) on MJO predictability and prediction, there have been several review articles focusing on the MJO (Zhang et al. 2013), subseasonal prediction (National Academies of Sciences, Engineering, and Medicine 2016), and ongoing international activities on MJO and subseasonal prediction (Robertson et al. 2015; Lee et al. 2017; Ling et al. 2017; Vitart et al. 2017; Wheeler et al. 2017a). These latter reviews provide broad views of the recent activities on MJO research and applications but do not focus on our recent gains in the science of MJO prediction. This paper will review the advances that have been made since Waliser (2011) regarding our MJO prediction capabilities with dynamical prediction systems and our scientific understanding of its predictability.

Therefore, the articles cited here are mainly those published after 2010. Although the northward-propagating boreal summer intraseasonal oscillation is considered as a dominant subseasonal mode during the summer, it is not within the scope of the current review.

An overview of international activities that have promoted the advancement of MJO prediction is introduced in section 2. Review of the metrics/measures used in the MJO prediction studies is provided in section 3, followed by a review of MJO predictability and prediction skill in the recent hindcasts in section 4. A detailed review of the factors that influence the MJO prediction skill is provided in section 5. Summary, remaining challenges, and suggestions are discussed in section 6, followed by conclusions in section 7. Acronyms are given in Table 1.

2. Multimodel experiments and field campaigns

There have been several internationally coordinated efforts on multimodel hindcast experiments with the aim of better understanding of the subseasonal predictability and prediction (Zhang et al. 2013). The Intraseasonal Variability Hindcast Experiment² (ISVHE) launched in 2009 was the first attempt to coordinate multimodel long-term hindcast experiments focusing on intraseasonal prediction, with a particular emphasis on multimodel ensemble approach that has been proven to be one of the most effective ways to improve the seasonal prediction (e.g., Palmer et al. 2000, 2004; Shukla et al. 2000) and MJO prediction (Kang and Kim 2010; Fu et al. 2013). Eight ocean–atmosphere coupled models from six centers participated in this experiment (Neena et al. 2014). Hindcasts of at least 45-day forecast lead time were initialized on the 10th day of every month over about 20 years. The intraseasonal predictability and prediction skill from the ISVHE hindcasts have been documented in a series of papers (Zhang et al. 2013; Neena et al. 2014; Lee et al. 2015; Lee and Wang 2016).

The WWRP/WCRP Subseasonal to Seasonal Prediction Project³ (hereafter S2S Project) was launched in 2013, and the first phase will end in November 2018 (Zhang et al. 2013; Vitart et al. 2017), and the World Meteorological Organization (WMO) has now approved the S2S Project for a second phase of five years. Near-real-time forecasts and hindcasts from 11 operational centers have been delivered (Vitart et al. 2017) and are accessible to the research community from the ECMWF, CMA, or IRI data portals. By September 2017, 951 users from 92 countries have registered to the

¹ <http://www.cpc.ncep.noaa.gov/products/precip/CWlink/MJO/mjo.shtml>.

² <http://www.cgd.ucar.edu/projects/yotc/mjo/isvhe.html>.

³ <http://s2sprediction.net/>.

S2S database, and 225 TB (about 4 times the total volume of the S2S database) have been downloaded since May 2015.⁴ The majority of models demonstrated sub-seasonal skill improvement, compared to their earlier versions (Vitart 2017). MJO indices and associated forecast variables are produced in near real time (3-week delay)⁵ from centers participating in the S2S Project (Vitart et al. 2017).

Eleven models participated in the MJOTF/GASS multimodel experiment, producing 20-day hindcasts of two strong MJO events during the YOTC period in boreal winter 2009/10 (Klingaman et al. 2015a,b). From October 2011 to March 2012, international field campaign CINDY/DYNAMO (hereafter DYNAMO) collected in situ observations in the tropical Indian Ocean to investigate the mechanisms responsible for the initiation of the MJO (Yoneyama et al. 2013; Zhang et al. 2013). Three MJO events were captured by the radar, ship/mooring, and sounding observational network during the DYNAMO field campaign. Based on the in situ data, various aspects of the MJO have been documented. Several studies conducted hindcast experiments for the DYNAMO period to better understand the processes associated with the MJO and to assess the MJO prediction ability in global and regional models (e.g., Fu et al. 2013; Kerns and Chen 2014; Ling et al. 2014; Hannah et al. 2015; Xiang et al. 2015; Hagos et al. 2016; Janiga and Zhang 2016), which will be discussed in section 4.

3. Forecast and verification metrics

a. MJO index

The most popular index used for MJO prediction studies is the Real-time Multivariate MJO (RMM) index developed by Wheeler and Hendon (2004). RMM1 and RMM2 are the first and second principal components of the combined empirical orthogonal functions (EOFs) of outgoing longwave radiation (OLR), zonal wind at 200 and 850 hPa averaged between 15°N and 15°S. Figure 1 is an update of Wheeler and Hendon (2004, their Fig. 8) using ERA-Interim (Dee et al. 2011) and NOAA OLR (Liebmann and Smith 1996) from 1979 to 2017. It represents the observed MJO life cycle in eight different phases (phases 1–8) by compositing the OLR and 850-hPa horizontal wind anomalies from December to February (DJF) without discrimination for MJO amplitude. The predicted RMMs are obtained by

TABLE 1. List of acronyms.

Acronyms	
20CRv2C	NOAA Twentieth Century Reanalysis v2C
BCC	Beijing Climate Center
BoM	Bureau of Meteorology (Australia)
CAM	Community Atmosphere Model
CESM	Community Earth System Model
CFS	Climate Forecast System
CMA	China Meteorological Administration
CPC	Climate Prediction Center
CYNDY	Cooperative Indian Ocean Experiment on Intraseasonal Variability in Year 2011
DYNAMO	Dynamics of the MJO
ECCC	Environment and Climate Change Canada
ECMWF	European Centre for Medium-Range Weather Forecasts
ERA-Interim	ECMWF interim reanalysis
FIM-iHYCOM	Flow-following Icosahedral Model coupled with an icosahedral-grid version of the Hybrid Coordinate Ocean Model
GASS	Global Energy and Water Exchanges Atmospheric System Study
GEFS	Global Ensemble Forecast System
GEOS-5	Goddard Earth Observing System Model version 5
GFDL	Geophysical Fluid Dynamics Laboratory
GFS	Global Forecast System
GloSea5	Global Seasonal forecasting system version 5
IRI	International Research Institute for Climate and Society
MAPP	Modeling, Analysis, Predictions, and Projections
MJOTF	MJO Task Force
NASA	National Aeronautics and Space Administration
NCAR	National Center for Atmospheric Research
NCEP	National Centers for Environmental Prediction
NICAM	Nonhydrostatic Icosahedral Atmospheric Model
NOAA	National Oceanic and Atmospheric Administration
POAMA	Predictive Ocean–Atmosphere Model for Australia
SCOAR	Scripps Coupled Ocean–Atmosphere Regional
SNU	Seoul National University
SP-CAM	Super Parameterized Community Atmosphere Model
UH	University of Hawaii at Mānoa
UKMO	Met Office
WCRP	World Climate Research Programme
WWRP	World Weather Research Programme
YOTC	Year of Tropical Convection

the projection of the predicted anomalies onto the observed combined EOF eigenvectors. More details on the procedure can be found in Gottschalck et al. (2010) and Vitart (2017). NOAA/CPC and the S2S Project provide

⁴ http://s2sprediction.net/file/documents_reports/Minutes_6th_SGM.pdf.

⁵ http://gpvjma.ccs.hpc.jp/S2S/S2S_MJO.html.

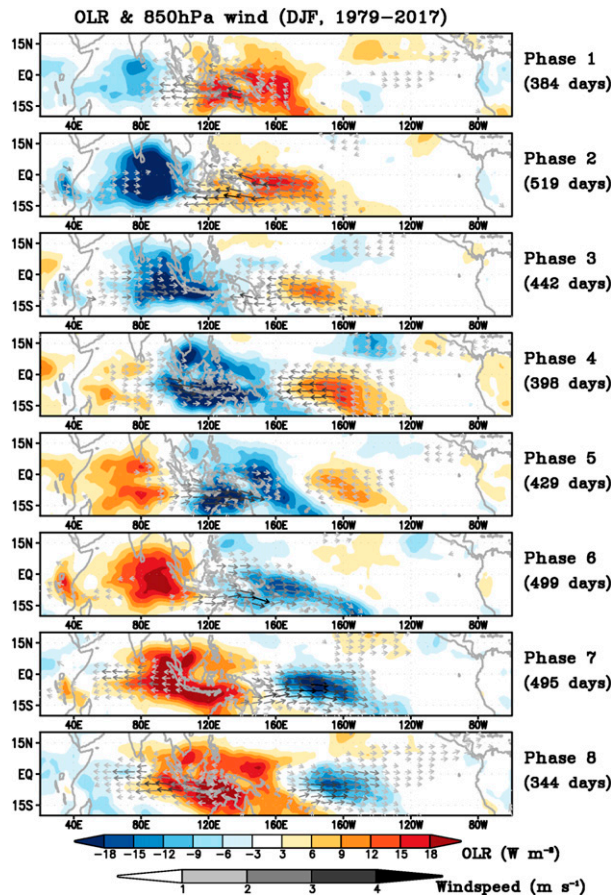


FIG. 1. DJF composite for OLR (W m^{-2} ; shading) and 850-hPa wind vector anomalies and wind speed (m s^{-1} ; shading) anomalies calculated for eight MJO phases from 1979 to 2017. The number of days falling within each phase is given.

RMM forecasts on the phase–space diagram (Wheeler and Hendon 2004), which represents the location (phase) and amplitude of the MJO as a function of forecast lead times.

The majority of the studies on MJO simulation and forecasts use the RMM index as a measure of the MJO. Although the RMM index is relatively simple to calculate and thus, easy to implement for real-time monitoring and forecasting, interpretation of the results often requires careful consideration. A principal weakness of the RMM index is that the fractional contribution of zonal wind fields to the variance of RMMs is considerably larger than the contribution of the convective fields (e.g., Straub 2013). Therefore, RMM skill mainly reflects the skill of the predicted wind anomalies but not necessarily the predicted convective anomalies (i.e., precipitation or OLR; Kim et al. 2014; Klingaman et al. 2015a). In other words, although the models do not predict the convective anomaly very well (e.g., the eastward propagation of the MJO precipitation), the

prediction skill measured by the RMM could result in fairly high skill, leading to a more optimistic conclusion regarding our MJO prediction capabilities. Several alternative methods have been introduced (e.g., Ventrice et al. 2013; Kiladis et al. 2014; Ling et al. 2014; Kerns and Chen 2016; Liu et al. 2016; Zhang and Ling 2017), although the RMM index is being used in most MJO prediction studies and operational forecasts.

b. Prediction and predictability metrics

Predictability is the theoretically achievable skill with a perfect model, whereas prediction skill is an actual achievable skill in a given prediction system that contains initial condition and modeling errors. The difference between the predictability and prediction skill can be interpreted as a deficiency in the forecast system and provides an estimate of how much skill we might expect to gain by reducing the model error and by improving initial conditions. Common metrics that have been used in recent studies to measure the prediction skill and predictability of the MJO are reviewed. When comparing predictability and prediction skill in different models, caution should be exercised, as the hindcast period and season, ensemble size, verification dataset, and RMM computation procedure are usually not the same.

1) PREDICTION SKILL

To represent an MJO prediction skill of a forecast system, a common benchmark to measure the MJO performance is scalar metrics, such as the bivariate anomaly correlation coefficient (COR) or bivariate root-mean-square error (RMSE), which represents the skill as a function of forecast lead times (e.g., Lin et al. 2008; Rashid et al. 2011). COR and RMSE are calculated between the predicted and observed RMMs as follows:

$$\text{COR}(\tau) = \frac{\sum_{t=1}^{t=N} [a_1(t)b_1(t, \tau) + a_2(t)b_2(t, \tau)]}{\sqrt{\sum_{t=1}^{t=N} [a_1^2(t) + a_2^2(t)]} \sqrt{\sum_{t=1}^{t=N} [b_1^2(t, \tau) + b_2^2(t, \tau)]}},$$

RMSE(τ)

$$= \sqrt{\frac{1}{N} \sum_{t=1}^N [|a_1(t) - b_1(t, \tau)|^2 + |a_2(t) - b_2(t, \tau)|^2]},$$

where $a_1(t)$ and $a_2(t)$ are the verification (observation or reanalysis) RMM1 and RMM2 at time t , $b_1(t, \tau)$ and $b_2(t, \tau)$ are the respective forecasts for time t with a lead time of τ days, and N is the number of predictions. COR is equivalent to a spatial pattern correlation between

observation and forecast when they are reconstructed from the two leading EOFs (Lin et al. 2008). COR 0.5 is usually being used as a threshold of skill, approximately corresponding to a standardized RMSE of $\sqrt{2}$ for the bivariate RMM index (Rashid et al. 2011). Unless otherwise stated explicitly, the RMM prediction skill refers to the time at which the COR falls below 0.5. These performance-based metrics have been applied to subsets of forecasts, such as the forecasts initialized in various MJO phases or with different amplitudes (e.g., Rashid et al. 2011).

2) PREDICTABILITY

Prediction skill of a given forecasting system is limited by errors emanating from the imperfect model as well as the errors from the initial conditions. MJO predictability is regarded as an intrinsic limit of MJO prediction by assuming that the system has no error emanating from the model itself (and thus a perfect system), but only sensitive to the errors from initial conditions. The perfect-model approach provided a pathway to estimate predictability using dynamical models, although such predictability estimate is highly model dependent. The perfect-model assumption was first introduced in the MJO research with the twin ensemble experiment by Waliser et al. (2003), followed by several studies with multiensemble forecasting systems (Kim and Kang 2008; Pegion and Kirtman 2008; Neena et al. 2014; Kim et al. 2014; Liu et al. 2017).

Predictability is estimated in terms of the model ability of each ensemble member to forecast the events from the control (or ensemble mean) simulation. There have been two different approaches to evaluate the MJO predictability: one is the anomaly correlation metrics, and the other is the signal-to-noise metrics. The anomaly correlation metric computes the correlation between one ensemble member considered as the truth and the rest of the ensemble members (Buizza 1997; Pegion and Kirtman 2008; Kim et al. 2014; Xiang et al. 2015; Liu et al. 2017; Wheeler et al. 2017b). For example, MJO predictability is computed in the same way as the prediction skill (COR), but with correlating the RMM index from the control (or ensemble mean) with the selected ensemble member (Kim et al. 2014). In the signal-to-noise approach, the signal is defined as the variance of the ensembles within a certain temporal window that is large enough to encompass an entire MJO event (e.g., 50-day sliding window). Noise is estimated as the mean-square error of ensembles relative to the control experiment (single ensemble member or ensemble mean). Then, the predictability is defined as the forecast lead time when the noise exceeds the signal (Waliser et al. 2003; Kim and Kang 2008; Pegion and Kirtman 2008; Fu et al. 2013; Neena et al. 2014). Neena

et al. (2014) used the signal-to-noise approach to define the MJO prediction skill by replacing the control simulation with reanalysis.

3) AMPLITUDE AND PHASE

Basically, two factors can impact the MJO prediction skill and predictability: the amplitude and phase of the MJO. To identify the errors of the predicted amplitude and phase, most of the studies follow the metrics by Rashid et al. (2011). The MJO amplitude is defined as

$$\text{AMP}(t, \tau) = \sqrt{\text{RMM1}(t, \tau)^2 + \text{RMM2}(t, \tau)^2}.$$

The amplitude error measures how fast the forecast system loses the amplitude of the MJO signal and can be calculated simply by comparing the predicted with the observed amplitude as a function of lead time as

$$\text{ERR}_{\text{amp}}(\tau) = \frac{1}{N} \sum [\text{AMP}_{\text{prd}}(t, \tau) - \text{AMP}_{\text{obs}}(t)].$$

Negative (positive) $\text{ERR}_{\text{amp}}(\tau)$ indicates weaker (stronger) amplitude in predictions, compared to the observation. The phase error measures the difference of the angle between the predicted phase and observed phase in the RMM phase-space diagram. The phase angle error can be measured as a function of lead time as

$$\text{ERR}_{\text{phase}}(\tau) = \frac{1}{N} \sum \tan^{-1} \left[\frac{a_1(t)b_2(t, \tau) - a_2(t)b_1(t, \tau)}{a_1(t)b_1(t, \tau) + a_2(t)b_2(t, \tau)} \right].$$

Negative (positive) $\text{ERR}_{\text{phase}}(\tau)$ indicates slower (faster) propagation in predictions, compared to the observation.

4) PROBABILISTIC MJO FORECAST

Compared to the traditional metrics for MJO prediction and verification, the probabilistic forecast approach has received little attention to date. Very recently, Marshall et al. (2016) proposed a new display of ensemble predictions of the MJO for real-time forecast that overcomes some of the shortcomings in the traditional display that have been difficult in interpreting a dispersive ensemble plume. Also, forecast verification using probability-based skill scores (instead of deterministic skill measures) is introduced to evaluate the model performance (Marshall et al. 2016). Probabilistic forecasts have been recently implemented for the real-time forecast⁶ of the MJO at the Bureau of Meteorology, Australia.

⁶ http://poama.bom.gov.au/researcher/agm/project/mjo_prob/mjo_prob.html.

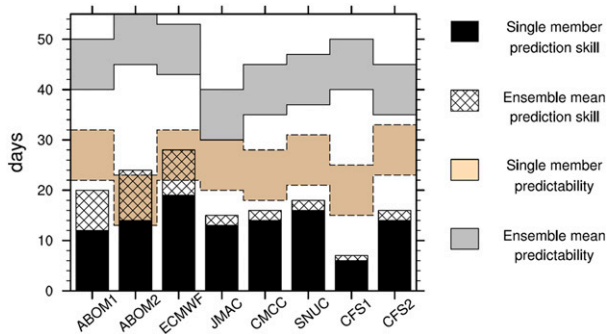


FIG. 2. The single-member prediction skill (black bar) and ensemble-mean prediction skill (hatched bar) estimates (days) for MJO for the eight models are shown along with their respective single-member (tan-shaded area) and ensemble-mean (gray-shaded area) estimates of MJO predictability [± 5 -day range; Fig. 4 from Neena et al. (2014)].

4. MJO predictability, prediction skill, and predicted characteristics

a. MJO predictability

With the perfect-model approach, the predictability of the MJO has been known to be about 3–4 weeks when measured by intraseasonally filtered upper-level circulation field and about 2 weeks by filtered precipitation (Waliser et al. 2003; Liess et al. 2005). Such level of MJO predictability was later supported by various numerical model experiments (Reichler and Roads 2005; Kim and Kang 2008; Pegion and Kirtman 2008). Studies argued that MJO predictability can be extended for several days when the ocean–atmosphere coupling process is included (Fu et al. 2007; Pegion and Kirtman 2008), although the negligible improvement was proven in others (Kim and Kang 2008). The models used in these predictability studies, however, were only marginally successful at simulating the MJO.

After those studies were published around 2008, MJO predictability study reached a plateau until 2014. Two papers published in 2014 have shown that with multimodel state-of-the-art forecasting systems, the MJO predictability can reach up to 6–7 weeks when defining the MJO with the RMM indices (Kim et al. 2014; Neena et al. 2014). Figure 2 shows the predictability and prediction skill from multimodels that participated in the ISVHE project (Neena et al. 2014). With the signal-to-noise approach, the predictability of the ensemble-mean RMM forecast in most of the models ranges from 35 to 45 days. ECMWF and ABOM2 exhibit a higher predictability of up to 45 days (Neena et al. 2014) and about 40 days in BCC (Wu et al. 2016).

With the anomaly correlation approach with RMMs, MJO predictability in ECMWF, NCEP CFSv2, GFDL,

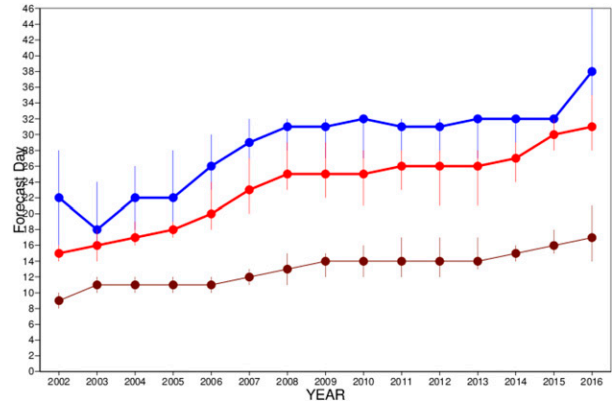


FIG. 3. Evolution of the MJO skill scores (RMM bivariate correlations) since 2002 in ECMWF hindcasts. The MJO skill scores have been computed on the ensemble mean of the ECMWF hindcasts produced during a complete year. The blue, red, and brown lines indicate the day when the MJO bivariate correlation reaches 0.5, 0.6, and 0.8, respectively [updated Fig. 1 from Vitart (2014)].

and POAMA remains above 40 days (Rashid et al. 2011; Kim et al. 2014; Xiang et al. 2015; Marshall et al. 2017), but is limited to 30 days in the BCC (Liu et al. 2017). The consensus among the studies listed above is that the initially stronger MJO events tend to be more predictable. The predictability for initially strong MJO events ranges from 35 to 45 days, while for initially weak MJO it is around 20–30 days (Neena et al. 2014; Wu et al. 2016). Although the predictability is shown to be dependent on the initial amplitude of the MJO, it is not sensitive to initial phases (Kim et al. 2014; Neena et al. 2014; Wu et al. 2016; Liu et al. 2017).

b. MJO prediction skill

The ensemble-mean RMM prediction skill scores (measured by signal-to-noise metrics) in the ISVHE hindcasts vary widely, between 1 and 4 weeks in the boreal winter, with the majority of the models having skill of 2–3 weeks (Fig. 2). It needs to be mentioned that these ISVHE hindcasts were produced around 2009 (Neena et al. 2014). During the past decade, some forecasting systems have shown a substantial improvement in MJO prediction. For example, MJO skill in CFSv2 (~3 weeks; Wang et al. 2014) has been significantly extended, compared to its previous version, CFSv1 (~1.5 weeks; Seo et al. 2009). Figure 3 shows the evolution of the RMM skill score in ECMWF measured with the ensemble-mean hindcasts and ERA-Interim. Since 2002, an average gain of skill is about 1 day per year from 2002 to 2011 (Vitart 2014). The flat correlation 0.5 curve between 2013 and 2015 is because the forecast lead time was limited to 32 days until 2015, but extended to 46 days since May 2015. Continuous

improvement of RMM skill in ECMWF has been attributed to the reduction of the amplitude and phase error (Vitart 2014). POAMA and UKMO have also shown MJO skill improvement (Rashid et al. 2011; Neena et al. 2014; Marshall et al. 2017; MacLachlan et al. 2015).

The recent S2S Project hindcasts have RMM prediction skill scores varying widely between 10 and 38 days (Fig. 4), with a similar range of skill in the recent SubX hindcasts (K. Pegion 2018, meeting presentation⁷), which exhibit an overall improvement over the ISVHE models. In addition to the ISVHE and S2S Project hindcasts (made up of operational models), studies have shown the MJO prediction skill in various models. About 4 weeks of RMM skill have been demonstrated in the GFDL (Xiang et al. 2015) and NICAM model (Miyakawa et al. 2014) in boreal winter; about 3-week skill in BCC (Liu et al. 2017) and FIMiHYCOM (Green et al. 2017) in all seasons; and about 2 weeks in the atmosphere-only models, such as GEFS (Hamill and Kiladis 2014) and BCC (Wu et al. 2016).

Besides the long-term hindcast simulations, forecast experiments have been performed on individual MJO events during a specific period. For the two strong MJO events during the YOTC period (October 2009–January 2010), the majority of models have proven RMM skill (correlation 0.7) of two weeks, with several models maintaining skills beyond that (Klingaman et al. 2015a). For the DYNAMO period (September 2011–March 2012), the RMM skill (correlation 0.5) is about 13 days in GFS, 22 days in CFSv2, 27 days in BCC, 28 days in UH, and 29 days in the GFDL model (Fu et al. 2013; Xiang et al. 2015; Liu et al. 2017). With relatively short forecast experiments for the DYNAMO period, the RMM skill (correlation 0.9) is 9 days in SPCAM, 7 days in NCAR CAM5 (Hannah and Maloney 2014; Hannah et al. 2015), and 5 days in NICAM (Nasuno 2013).

c. MJO characteristics in hindcasts

1) MJO AMPLITUDE

MJO amplitude and phase are both important in the assessment of MJO prediction skill. The majority of the contemporary models exhibit faster decay of the MJO signal than the observation. Even though the forecasts are initialized with a strong MJO signal, the predicted MJO signal does not persist as long as it does in observations. By comparing two operational forecasting systems, NCEP CFSv2 and ECMWF (version cy32r3), Kim et al. (2014) showed that the amplitude of the initially

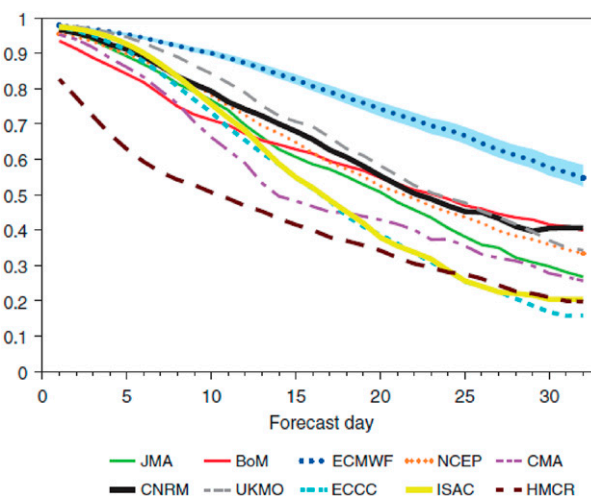


FIG. 4. RMM bivariate correlation between the model ensemble means and ERA-Interim for 10 S2S models [Fig. 1 from Vitart (2017)].

strong MJO events (RMM amplitude > 1.5) is kept above a strong category (> 1.5) until 10 days in both observation and in NCEP CFSv2, while the ECMWF drops to its threshold (1.5) in a week. Fast decay of the MJO amplitude is also shown in the POAMA (Rashid et al. 2011), GFDL (Xiang et al. 2015), and BCC (Wu et al. 2016; Liu et al. 2017). The majority of the S2S Project hindcasts tend to lose the MJO amplitude faster than the observed within a week (Fig. 5a; Vitart 2017). The change of amplitude varies among initial MJO phases, while there is no consensus of the amplitude dependency on initial phases among models. For example, the amplitude decreases faster than other phases when the model is initialized at phases 2–3 in NCEP CFSv2 and ECMWF (Kim et al. 2014), at phases 3–4 in POAMA (Rashid et al. 2011), and at phases 4–6 in BCC (Liu et al. 2017) and GFDL (Xiang et al. 2015).

2) MJO PHASE

In general, during boreal winter, the MJO convection envelope tends to initiate in the Indian Ocean and propagate across the Maritime Continent to the western Pacific. Skill declines are attributed to phase errors (Lim et al. 2018) rather than to amplitude errors, meaning that the propagation (or stagnation) of the MJO is not accurately predicted (Rashid et al. 2011; Kim et al. 2014; Vitart 2014; Wang et al. 2014; Xiang et al. 2015; Wu et al. 2016; Liu et al. 2017). A consensus among studies is that models present slower propagation speed than the observed. There is about a 2-day delay, on average, over a 30-day lead time forecast in POAMA (Rashid et al. 2011). MJO propagation in the ECMWF and NCEP CFSv2 is about 15° longitude slower than observation over a 25-day forecast lead

⁷ <https://ams.confex.com/ams/98Annual/meetingapp.cgi/Paper/331093>.

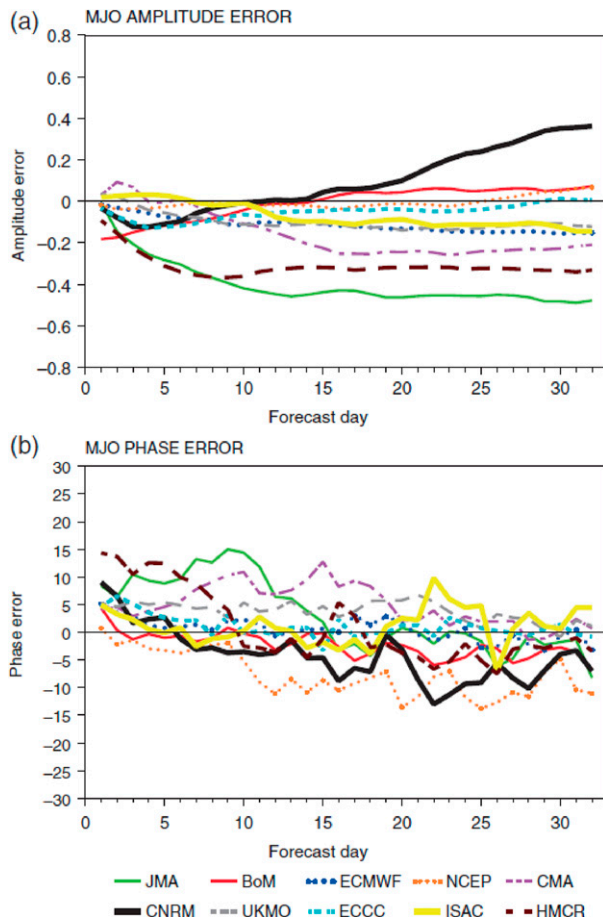


FIG. 5. Evolution of the MJO (a) amplitude error and (b) phase error relative to ERA-Interim as a function of lead time. In (a), a positive (negative) value indicates a too strong (weak) MJO. In (b), a positive (negative) value indicates a too fast (slow) MJO propagation [Fig. 3 from Vitart (2017)].

time (Kim et al. 2014). In most of the S2S Project hindcasts, the phase error changes to negative (slower propagation) after about 2 weeks (Fig. 5b; Vitart 2017). On the contrary, some models (GFDL and BCC) have shown rather faster propagation (Xiang et al. 2015; Liu et al. 2017). Although the phase error varies among initial phases, there is no consensus of the phase error dependency on initial phases among models.

Most forecast systems have some deficiencies in predicting the MJO propagation through the Maritime Continent, a problem referred to as the Maritime Continent MJO prediction barrier (Vitart et al. 2007; Seo et al. 2009; Seo and Wang 2010; Vitart and Molteni 2010; Wang et al. 2014; Kim 2017; Vitart 2017). This barrier is likely not an inherent predictability issue but rather a modeling issue due to poor representation of the MJO propagation (Kim et al. 2014; Neena et al. 2014). This will be discussed in section 6.

5. Sensitivity of MJO prediction skill to various factors

It is obvious that MJO prediction skill has significantly extended during the last decade. However, a significant gap between our demonstrated prediction skill measures and our estimates of predictability still remains. In this section, various factors that are shown to impact MJO prediction skill are reviewed.

a. MJO amplitude and phase

MJO prediction skill is sensitive to the initial amplitude and phase of the MJO. When the model is initialized with a strong MJO signal, the prediction skill (correlation coefficient) tends to be higher than when initialized with weak or with no MJO signal (e.g., Kim et al. 2014; Lim et al. 2018). Skill is higher in boreal winter when the MJO is generally more active (e.g., Rashid et al. 2011; Wang et al. 2014; Liu et al. 2017; Lim et al. 2018). In the S2S Project hindcasts, the average skill of the initially moderate MJO events lies in between the strong and weak events (Fig. 6). Although recent studies have agreed on the MJO skill–amplitude relationship, skill does not seem to improve gradually as the MJO amplitude becomes stronger. For example, Kim et al. (2016) found that not all initially weak MJO events have low skill, and not all strong MJO events result in high skill. The predictions starting with moderate MJO amplitude especially could either end up with high or low skill depending on the environmental condition, which eventually induces favorable (or unfavorable) conditions for MJO development.

MJO prediction skill largely depends on the phase of the MJO. When a forecast is initialized in a specific phase of the MJO, the skill can be higher than other phases. However, among recent studies, there is no consensus about the MJO skill–phase relationship. For example, ECMWF (Fig. 7) and GFDL hindcasts show relatively high skill when the model is initialized with an MJO signal in the Indian Ocean (phases 2–3; Xiang et al. 2015; Kim 2017), but in phases 3–4 in POAMA (Rashid et al. 2011) and phases 4–5 and phases 8–1 in CFSv2 (Wang et al. 2014). The sensitivity of prediction skill to the initial MJO phases is highly model dependent. In the most recent S2S Project hindcasts, there is no consensus found for MJO skill–phase dependency (Lim et al. 2018).

b. Impact of the mean state and extratropics

MJO predictability and prediction skill varies with changes in the low-frequency background and/or mean state (e.g., Waliser et al. 2001). With 30-yr hindcasts from the POAMA, a substantial extension of the MJO

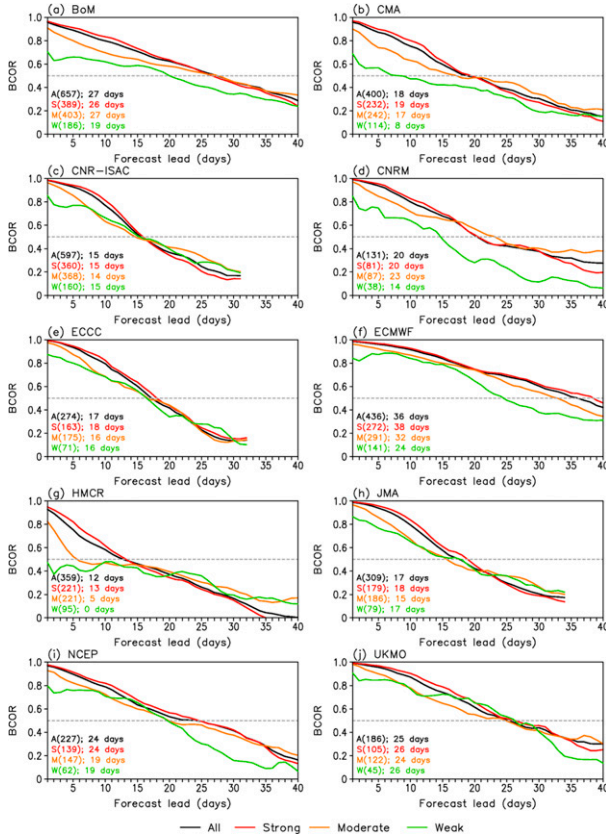


FIG. 6. RMM bivariate correlation of each S2S model as a function of forecast lead times for all reforecasts (A; black), and those initialized during strong (S; red), medium (M; orange), and weak MJO events (W; green). The number of reforecasts used in each category and their prediction skill are indicated at the bottom-left corner [Fig. 2 from Lim et al. (2018)].

predictability and prediction skill is found during the easterly phase of the quasi-biennial oscillation (QBO; Marshall et al. 2017). The RMM prediction skill is 31 days in the easterly QBO years, but only 23 days in the westerly QBO years. The extended prediction skill and predictability during the easterly QBO are not only due to more initially stronger MJO events (Yoo and Son 2016; Son et al. 2017), but also to a more coherent MJO event (Nishimoto and Yoden 2017). Besides the QBO, MJO prediction skill is sensitive to the Indian Ocean dipole (IOD). In the 20-yr hindcasts from BCC, RMM prediction skill is about 15 days during negative IOD years but extends to 20 days during positive IOD years (Liu et al. 2017). However, this RMM skill–IOD relationship is not rooted in the observed physical processes between the MJO and IOD, but is mainly due to the mean state bias. Besides the studies by Waliser et al. (2001), Marshall et al. (2017), and Liu et al. (2017), the interannual change of MJO prediction has received

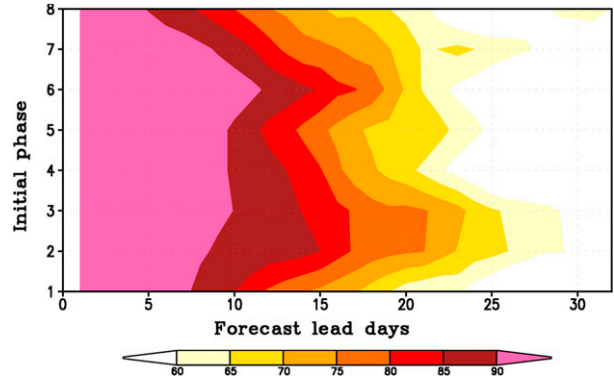


FIG. 7. RMM bivariate correlation for ensemble mean by initial phases for strong MJO cases in the ECMWF hindcasts. Correlation coefficients are multiplied by 100 [Fig. 1b from Kim (2017)].

little attention, mainly due to the lack of hindcasts over a sufficiently long period. A better understanding of the large-scale basic state forcing on MJO predictability could potentially enhance the MJO prediction skill.

In addition to the tropical mean state, the extratropical circulation influences MJO prediction. Using a series of relaxation hindcast experiments with the ECMWF model, Vitart and Jung (2010; cf. Ferranti et al. 1990) showed that the RMM skill drops significantly from 28 to 22 days when the extratropical influence on tropics is artificially suppressed. This is mainly due to a slower propagation speed and weaker MJO amplitude, consistent with Ray and Li (2013). In contrast, RMM skill increases from 28 to 40 days when the extratropics are relaxed toward the ERA-Interim. More work is needed to better understand the extratropical influence on MJO prediction as a source of predictability.

c. Ensemble generation

In weather and climate prediction, there has been an increasing use of ensembles to obtain better forecasts. One advantage of using ensembles is that the forecast uncertainty can be estimated via ensemble spread (ensemble standard deviation). For a perfectly reliable system, the ensemble spread equals the RMSE between the ensemble mean and observation (e.g., Leutbecher and Palmer 2008). Ensemble predictions for MJO have been shown to be underdispersive (or overconfident), indicating lack of ensemble spread (Rashid et al. 2011; Kim et al. 2014; Neena et al. 2014; Xiang et al. 2015; Green et al. 2017; Liu et al. 2017; Lim et al. 2018). Figure 8 shows the relationship between the ensemble spread and the ensemble-mean RMSE for the MJO in ISVHE hindcasts (Neena et al. 2014). In all models, the spread is smaller than the RMSE, and models with

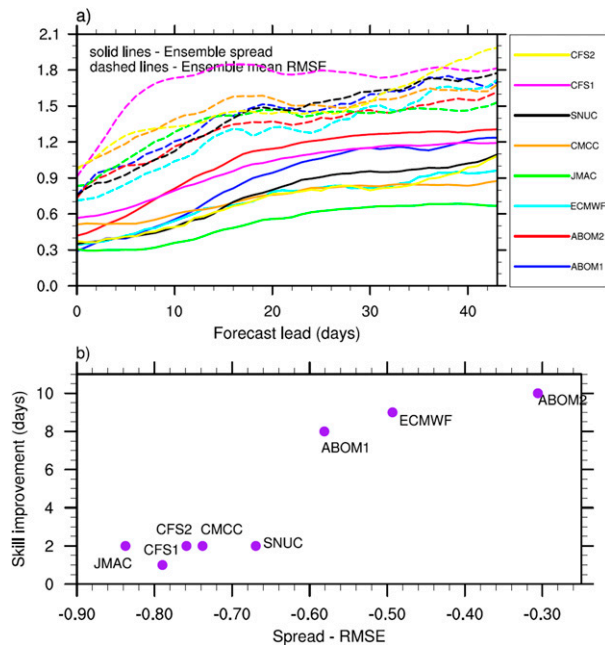


FIG. 8. (a) Bivariate measure of ensemble spread (solid lines) and ensemble-mean RMSE (dashed lines) for the MJO in the different ensemble prediction systems. (b) The 25-day forecast lead average of the spread minus RMSE values [set of solid and dashed curves in (a)] for each model, plotted against the corresponding values of skill improvement (day) in ensemble means over single-member forecasts [Fig. 5 from Neena et al. (2014)].

relatively better-dispersed ensembles exhibit higher ensemble-mean skill (Fig. 8b).

Several efforts are underway to improve the representation of uncertainties from initial conditions and the models. To generate initial perturbations suitable to MJO prediction, the breeding method (Liess et al. 2005; Chikamoto et al. 2007) and singular vectors (Molteni and Palmer 1993; Ham et al. 2012) have been explored/adopted. With 10-yr hindcasts using NASA GEOS-5, Ham et al. (2012) showed 2–3-day extended RMM skill with an empirical singular vector approach than random perturbations. With the SNU GCM hindcast, RMM skill does not substantially differ among three different perturbation methods (Kang et al. 2014). There have also been efforts toward improving the representation of uncertainty in the model physics schemes. For example, in the ECMWF Ensemble Prediction System, the stochastic perturbation schemes improved the frequency and amplitude of the MJO (Weisheimer et al. 2014) and the spread–error relationship (Palmer et al. 2009; Leutbecher et al. 2017; Subramanian and Palmer 2017). In addition to improving the models, devising ensemble generation approaches tailored for the MJO might have a considerable impact on MJO prediction.

d. Multimodel ensemble forecasting

Recent studies have clearly shown that averaging multiensembles or multimodels can extend the MJO prediction skill (e.g., Fu et al. 2013; Kim et al. 2014; Neena et al. 2014; Ren et al. 2017). In all models, ensemble-mean skill exceeds single ensemble member skill in MJO prediction (e.g., Fig. 2 and Neena et al. 2014). The size of the ensemble also impacts the ensemble-mean skill. Vitart (2017) showed that in ECMWF hindcasts, RMM skill (correlation 0.6) can be reached at 28 days instead of 25 days when using 11 ensemble members instead of five members. The S2S models with relatively larger ensemble size show greater improvements of RMM skill in ensemble mean, compared to their control forecasts (Vitart 2017).

With an equally weighted multimodel ensembles (MME) of CFSv2 and UH hindcasts, a significant extension of RMM skill (36 days) was found, compared to their individual skills (22 and 28 days, respectively; Fu et al. 2013). By averaging two GCMs and one statistical model with different weightings, RMM skill can be sustained about 4–5 days longer than the best dynamical model (Kang and Kim 2010). When two dynamical models with similar prediction skill and sufficient model diversity are combined, the MME shows improvements in RMM skill, although including a low-performance model in the MME can degrade the skill (Green et al. 2017). Combining all available hindcasts with an equal weighting for an MME does not exceed the skill of averaging a few good models (Zhang et al. 2013). To extend the MJO skill, therefore, the individual model needs to be improved in tandem with developing an optimal strategy for MME.

e. Ocean–atmosphere coupling

The ocean–atmosphere interaction affects the MJO simulation and prediction. Many observational diagnoses have shown coherent variations in sea surface temperature (SST), surface fluxes, and convection associated with the MJO [review by DeMott et al. (2015) and references therein]. Particularly in the Indo-Pacific Ocean, warm SST east of the MJO convection supports the MJO propagation by affecting SST-modulated heat fluxes and enhancing the boundary layer moisture convergence, which maintains the convective anomalies and fuels the eastward propagation (e.g., Lindzen and Nigam 1987; Waliser et al. 1999; Maloney and Sobel 2004; Back and Bretherton 2009; Hsu and Li 2012; Hirata et al. 2013).

The importance of such ocean feedback to MJO forecast has been demonstrated in several studies. In hindcasts over short periods during major field campaigns,

about a 3–5-day improved MJO skill was found in the coupled configuration, compared to the uncoupled forecasts in the NCEP CFSv1 (Seo et al. 2009), CFSv2 and ECHAM (Fu et al. 2013), and Met Office Unified model (Shelly et al. 2014). With hindcasts over a longer period (>10 years), turning off the coupled feedback resulted in a loss of 8 days of RMM skill in FIM-iHYCOM hindcasts (Green et al. 2017). When the model is initialized over the Indian Ocean, a 2–3-day extended RMM skill was found in the SNU coupled model due to the realistic simulation of the SST–convection quadrature relationship (Kim et al. 2010). With 20-yr ECMWF hindcasts, Kim et al. (2016) showed that the MJO event that results in high RMM skill has more realistic ocean–atmosphere feedback during its prediction than the low RMM skill event.

Using ECMWF hindcast experiments covering the TOGA COARE period, Woolnough et al. (2007) and Vitart et al. (2007) detected a 5-day improvement in RMM skill when the atmosphere is coupled to an ocean model, primarily from high vertical resolution (1 m) in the near surface and high coupling frequency (hourly). It is demonstrated that the vertical mixing processes play an important role in determining the intraseasonal and diurnal variation of the SST, which develop in response to the surface fluxes driven by the MJO convection. With hindcast experiments for the DYNAMO period using the high-resolution SCOAR model, Seo et al. (2014) also demonstrated the critical role of diurnal SST variability in the buildup of preconvection warming and moistening, indicating the diurnally varying SST as a source of the MJO predictability. A coarse vertical resolution (~10 m) for the upper ocean is probably not sufficient to resolve the intraseasonal to diurnal SST variability.

Although most studies show improvement in MJO prediction by including the ocean–atmosphere interaction, Hendon (2000) demonstrated that the coupling could degrade the MJO skill due to the error in the basic state. Moreover, the role of coupling is case dependent. Among five MJO events that occurred during DYNAMO, only two observed MJO events were strongly coupled with the ocean, while some of them are largely controlled by the atmospheric internal dynamics (Fu et al. 2015). The atmospheric response to the ocean also varies with the model physics (convective parameterization; Wang et al. 2015). Various aspects of the model configurations, such as model physics and resolution, could also affect the response of the MJO to ocean–atmosphere coupling (Seo and Wang 2010; Crueger et al. 2013).

f. Model physics and resolution

Due to the huge computational costs for a long record of extended range hindcasts experiment, only a

handful of studies have performed sensitivity tests of the MJO skill to model physics or resolution. Most of the studies are based on case studies. Using the operational GFS for the DYNAMO period, Wang et al. (2015) found the MJO forecasts to be sensitive to the cumulus convection scheme. In particular, the simplified Arakawa–Schubert version 2 (SAS2) convection scheme (Han and Pan 2011), which has been used in the NCEP operational GFS since 2011, leads to a much weaker MJO amplitude and lower forecasting skill than the relaxed Arakawa–Schubert (RAS; Moorthi and Suarez 1992, 1999) and SAS (used in the NCEP CFSv2) schemes. This is mainly due to the drier lower troposphere caused by a persistent weak shallow convective moistening and stronger drying associated with the deep convection in SAS2, which leads to less intense convective activity.

The significant increase of the MJO prediction skill in the ECMWF model (Fig. 3) was mainly due to the improved model physics (Vitart 2014), although the improvement cannot be tied to a single change of the forecast system. Some of the improvements can be attributed to the introduction of a parameterization of ice supersaturation in 2006, new radiation parameterization in 2007, and modified convective parameterization in 2008 (Vitart 2014). The enhancement of skill in 2008 (model version cy32r3; Bechtold et al. 2008) is mainly attributed to the convective parameterization modified in a way that the deep convection became more sensitive to environmental moisture instead of being controlled by the large-scale moisture convergence (Bechtold et al. 2008; Hirons et al. 2013a,b). In particular, significant improvement is found for the MJO events initialized in the Indian Ocean (Vitart 2014). With CAM5, which is the atmospheric component of the NCAR CESM1, sensitivity experiments were performed for two MJO events during the DYNAMO period (Hannah and Maloney 2014). They showed that the RMM skill increases from 12 to 20 days via an enhancement to the entrainment rate for deep convection, which tends to strengthen the MJO amplitude (Bechtold et al. 2008). Similar MJO skill improvement by increasing entrainment is found in the hindcast for the YOTC period (Klingaman and Woolnough 2014).

Another attempt to improve the MJO prediction is the use of a model with superparameterization. In this approach, in place of using a conventional cumulus parameterization, a 2D cloud-resolving model is embedded in a GCM grid box. By comparing the DYNAMO hindcast of CAM5 with superparameterized CAM (SP-CAM), Hannah et al. (2015) showed that the SP-CAM hindcasts have a more robust

representation of the MJO convection, compared to CAM5. The RMM correlation skill is higher in SP-CAM, but with larger RMSE than the CAM5, due to the strong systematic drift in the SP-CAM. Miyakawa et al. (2014) performed hindcasts during 2003–12 with the NICAM global system-resolving model (14-km mesh) and showed that the RMM skill (correlation 0.6) is about 27 days, which outperforms the majority of operational forecasts. However, the physical reason for why the resolving cloud system improves the MJO prediction remains elusive.

Similarly, because of the computational cost, only a few studies have investigated the sensitivity of MJO prediction skill to changes in model resolution. By comparing the MJO skill in ECMWF with four different atmospheric model horizontal resolutions (about 300, 200, 120, and 80 km), Vitart et al. (2007) showed some extended skill in the higher-resolution versions, but not a gradual improvement as the resolution becomes higher. Further, by comparing the model with 60- and 30-km horizontal resolution and 62 and 137 vertical levels in the ECMWF model, no sensitivity of MJO prediction skill was found.⁸ At present, the impact of the atmospheric model resolution on MJO skill seems to be marginal, compared to the impact of physical parameterization or ocean–atmosphere coupling (Vitart et al. 2007).

g. Initial condition and verification dataset

Only a few studies have tested the MJO prediction sensitivity to initialization. In BCC hindcasts (Ren et al. 2017), the MJO prediction skill becomes slightly better when moisture is included in the initialization. Ling et al. (2014) examined the sensitivity of MJO prediction skill to observations assimilated in the analysis with the ECMWF model for the DYNAMO period. Although the sounding data or atmospheric motion vector winds over the Indian Ocean were excluded in the data assimilation system, no significant change in RMM prediction skill was found.

When the atmospheric initial conditions are derived from a system using a similar atmospheric model (e.g., ERA-Interim and ECMWF hindcast), the initial shock is smaller than when using initial conditions derived from different models (Wheeler et al. 2017b). Similarly, in some models, the MJO skill is sensitive to the choice of the verifying analysis. For example, when the ECMWF hindcast is verified against 20CRv2C instead of ERA-Interim, RMM skill (correlation 0.6) drops from 28 to 25 days (Vitart 2017). In addition, the MJO

prediction skill is sensitive to the quality of initial conditions, especially the atmospheric initial conditions. The RMM prediction skill (correlation 0.5) in ECMWF increases from 14 to 16 to 18 days when the forecast system uses atmospheric initial conditions taken from ERA-15, ERA-40, and ERA-Interim, respectively, due to a better representation of the MJO in the ERA-Interim (Vitart et al. 2007; Dee et al. 2011). A similar conclusion has been made with the UH hindcasts (Fu et al. 2011). With BCC hindcasts, Liu et al. (2017) showed that the RMM skill increases from 16 to 18 days with more accurate atmospheric initial conditions and further increases to 22 days with better ocean initial conditions. These studies suggest that the improvements of quality of atmospheric and ocean analyses/reanalyses are conducive to extending MJO prediction skill.

6. Summary and recommendations

The review synthesizes the key advances in MJO prediction studies during the past decade. Theoretical studies, multimodel experiments, and field campaigns have led to a better understanding of the processes, which are critical to simulating the MJO in numerical models. This has guided improvements to numerical weather prediction models, particularly boundary layer, cumulus convection, and microphysics parameterizations, leading to significant advances in MJO prediction.

The recent models have shown MJO prediction skill scores (based on RMM correlation coefficient 0.5) varying widely between 2 and 5 weeks, depending on the model, as well as the initial MJO phases and amplitudes. When a model is initialized with stronger MJO signal, prediction skill tends to be higher than when initialized with a weaker signal. Although the ensemble predictions have been shown to be underdispersive (or overconfident), prediction skill can be extended by improving ensemble generation approach tailored for MJO prediction and by averaging multiensembles or multimodels. MJO prediction skill can be influenced by the tropical mean state and low-frequency climate mode variations (QBO and IOD), as well as by the extratropical circulation. MJO prediction skill is proven to be sensitive to model physics, ocean–atmosphere coupling, and quality of initial conditions, while the impact of the model resolution seems to be marginal.

With the perfect-model approach, the estimate of the MJO predictability is 6–7 weeks, suggesting that many challenges remain to improve the dynamical forecasting systems and to fully realize the predictability of the MJO. Along with forecast system improvement

⁸ [ftp://cola.gmu.edu/pub/stan/MJOWorkshop/Vitart_MJO.pdf](http://cola.gmu.edu/pub/stan/MJOWorkshop/Vitart_MJO.pdf).

highlighted in previous sections, some additional specific issues and recommendations are discussed below.

a. Maritime Continent prediction barrier

The Maritime Continent is the largest archipelago on the planet, with complex land–sea distribution and orography and multiscale ocean–atmospheric interactions. When the MJO propagates from the Indian Ocean to the western Pacific, it often weakens or completely breaks down when it reaches the Maritime Continent (e.g., Rui and Wang 1990; Hendon and Salby 1994) due to orography, strong diurnal convection, disrupted atmosphere–ocean feedbacks, and many other factors. Compared to nature, this Maritime Continent barrier effect is exaggerated in climate models. In the earlier version of the ECMWF hindcast, Vitart et al. (2007) showed that the system does not accurately predict the MJO propagation through the Maritime Continent. Similar results were found in more recent versions of the ECMWF (Kim et al. 2014, 2016; Kim 2017; Vitart 2017), NCEP CFSv1 (Seo and Wang 2010; Fu et al. 2011), NCEP CFSv2 (Kim et al. 2014; Wang et al. 2014), GFDL (Xiang et al. 2015), and BCC (Liu et al. 2017) hindcasts. As mentioned before, studies have suggested that the Maritime Continent prediction skill barrier is a modeling problem, rather than a predictability issue (Kim et al. 2014; Neena et al. 2014).

Figure 9 shows the percentage of MJO events not crossing the Maritime Continent in the ERA-Interim and in 10 S2S Project hindcasts when the forecasts are initialized with strong MJO convection over the Indian Ocean (phase 2 or 3; Vitart 2017). The percentage is only about 10% in the ERA-Interim, but significantly higher in all the S2S Project hindcasts, with a proportion ranging from 19% to 46%. This indicates that simulating the MJO propagation across the Maritime Continent is one of the major hurdles to overcome to improve the MJO prediction skill. Because of the existence of this barrier in dynamical models, there has been a growing interest in understanding the critical processes involved in the MJO propagation, such as the Years of the Maritime Continent⁹ (YMC) international project.

b. Process-based hindcast evaluation

Many GCMs still exhibit shortcomings in simulating realistic MJO characteristics, including its amplitude, propagation, and horizontal and vertical structures (e.g., Jiang et al. 2015, 2018; Ahn et al. 2017). During recent years, great efforts have been made to understand the critical processes for better MJO simulation by

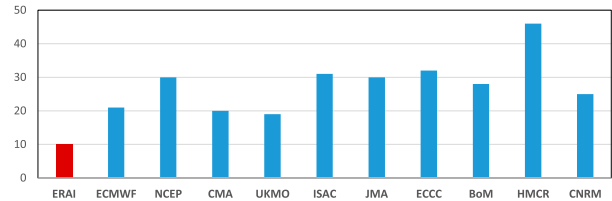


FIG. 9. Percentage of MJO events that are located in phases 2 or 3 (active phase over the Indian Ocean) in the initial condition with an amplitude larger than 1, which never propagate into the western Pacific (phases 6 or 7), even as a weak MJO during the following 30 days [modified from Table 1 of Vitart (2017)].

developing a so-called “process-based diagnosis” of GCMs [review by Jiang and Kim (2017)]. Several process-based metrics have been developed and applied to multiyear climate runs (e.g., Jiang et al. 2015; Ahn et al. 2017) and MJO hindcasts with case studies (Ling et al. 2014; Hannah et al. 2015; Klingaman et al. 2015a).

Up until now, however, evaluations of MJO fidelity in subseasonal forecasts have focused mostly on performance-based skill (e.g., correlation, RMSE) rather than on process-based metrics (e.g., moisture–convection process, convection–radiation feedback, ocean–atmosphere interaction). The lack of robust process-based studies in MJO prediction research was partly due to the lack of multiple variables output required for process study from frequently initialized hindcasts over a long period of time (>10 years). A newly launched multi-model subseasonal forecast effort is the Subseasonal Experiment¹⁰ (SubX), a NOAA Climate Test Bed project that combines multimodels from NOAA, NASA, the U.S. Navy, and ECCO to produce real-time forecasts as well as hindcasts, with a focus on subseasonal forecasts. In addition to the S2S Project, hindcast/forecast output from the SubX project, which will make available numerous fields from the current generation prediction systems, presents an unprecedented opportunity to relate MJO performance to process-based metrics. Such analysis will shed light on which physical processes in the atmosphere–ocean system need to be better represented in numerical models to produce better MJO predictions.

c. Mean state and MJO simulation fidelity

There is a growing interest in understanding the role of the mean state bias on MJO prediction. Biases in hindcasts/forecasts over the tropics develop quickly and become saturated within 5 days (e.g., Agudelo et al. 2009). Mean biases can distort the MJO skill scores by

⁹ <http://www.bmkg.go.id/ymc/>.

¹⁰ <http://cola.gmu.edu/kpegon/subx/>.

influencing further development of the MJO (Hannah et al. 2015; Kim 2017). From the moisture mode theory view (e.g., Raymond and Fuchs 2009; Sobel and Maloney 2012, 2013; Adames and Kim 2016), it has been argued that the horizontal moisture advection tends to play a dominant role in the eastward propagation of the MJO through the Maritime Continent. The advection of the seasonal mean moisture by the MJO-associated wind anomalies plays a particularly important role (Jiang et al. 2015, 2018; Adames and Kim 2016; Jiang 2017). Using model output from the MJOTF/GASS multimodel comparison project, Gonzalez and Jiang (2017) showed that the model fidelity in representing the mean moisture distribution over the tropical Indo-Pacific is strongly related to the MJO propagation fidelity. In other words, models with dry bias in the Indo-Pacific weaken the mean horizontal moisture gradient, thus dampening horizontal moisture advection associated with the MJO propagation. Similarly, by comparing individual moist static energy budget terms in the 20-yr ECMWF hindcast, Kim (2017) showed that the dry bias in the seasonal mean moisture field is a key factor that deteriorates the propagation and thus the prediction skill of MJO. The majority of S2S Project hindcasts have mean dry bias in the Indo-Pacific region, especially near the Maritime Continent (Lim et al. 2018). Understanding the role of mean state bias on MJO prediction and improving the mean state is crucial to extending the MJO prediction skill.

However, although a few studies argued that the systematic mean bias plays a role in MJO prediction, how the MJO–mean state tradeoff issue can be reconciled in the prediction point of view is unclear. A major issue that has plagued the modeling community for decades is the MJO and mean state tradeoff issue (Kim et al. 2011; Kim and Maloney 2017). Changes in convection scheme can improve the MJO simulation, but often also lead to the degradation of the mean state. By comparing 10 AGCM simulations, Kim et al. (2011) showed that the seasonal mean precipitation is degraded when the MJO is better simulated, and vice versa. It indicates that in some cases, the MJO may have been improved for the wrong reasons. Because better simulation of mean state and interannual variability (e.g., ENSO) has often had higher priority than the intraseasonal variability in model development, and because of the complexity and diversity of mechanisms associated with MJO, the improvement of the MJO simulation has been delayed (Kim and Maloney 2017). More focus on the relationship between the mean state and representation of MJO processes warrants further studies to improve the MJO prediction toward its theoretical predictability.

In addition to the MJO–mean state tradeoff issue, the link between model performance in simulating MJO and that in forecasting MJO needs to be considered. MJO simulation performance does not necessarily translate into prediction performance, which is partially shown in a series of studies (Jiang et al. 2015; Klingaman et al. 2015a; Xavier et al. 2015). For example, Klingaman et al. (2015a) compared the MJO prediction skill in multimodels with 20-day hindcast simulation for two MJO events. Among 27 model MJOTF/GASS hindcasts, two CAM5 models have shown the best MJO prediction skill, while they displayed very weak MJO activity and thus, weak MJO fidelity in the 20-yr climate simulations (Klingaman et al. 2015a). Such contradicting results between simulation and prediction may be attributed to a nonlinear interaction between model error and initial value error, which could make the prediction uncertain. Thus, understanding the relationship between simulation fidelity and prediction skill of the MJO and further obtaining a reliable description on the uncertainty of forecast error is a highly challenging task.

7. Conclusions

Subseasonal forecasts are particularly important since many management decisions, including those related to water, food, and hazard considerations, fall into this range. Skillful predictions of anomalous weather events, such as extreme precipitation and heat waves, in the subseasonal time scale could provide policy makers, emergency managers, and stakeholders with advanced warning to prepare mitigating actions. Since the MJO is regarded as a major source of subseasonal predictability, the continuous improvement of MJO prediction during the past decades warrants an optimistic view on forecasting for MJO-related extreme and hazardous, as well as fair weather, events. In particular, the recent collaborative efforts on subseasonal prediction (e.g., S2S Project, NOAA SubX, and NOAA S2S Task Force) provide an unprecedented opportunity to facilitate addressing the challenges with process-level understanding for MJO and associated weather and climate events.

Acknowledgments. Constructive and valuable comments from three anonymous reviewers are greatly appreciated. Kim was supported by NSF Grant AGS-1652289, NOAA Grant NA16OAR4310070, and the KMA R&D Program Grant KMI2018-03110. D. Waliser's contributions were carried out on behalf of the Jet Propulsion Laboratory, California Institute of Technology, under a contract with NASA, including support from the NASA Modeling, Analysis and Prediction Program.

REFERENCES

- Adames, Á. F., and D. Kim, 2016: The MJO as a dispersive, convectively coupled moisture wave: Theory and observations. *J. Atmos. Sci.*, **73**, 913–941, <https://doi.org/10.1175/JAS-D-15-0170.1>.
- Agudelo, P. A., C. D. Hoyos, P. J. Webster, and J. A. Curry, 2009: Application of a serial extended forecast experiment using the ECMWF model to interpret the predictive skill of tropical intraseasonal variability. *Climate Dyn.*, **32**, 855–872, <https://doi.org/10.1007/s00382-008-0447-x>.
- Ahn, M. S., and Coauthors, 2017: MJO simulation in CMIP5 climate models: MJO skill metrics and process-oriented diagnosis. *Climate Dyn.*, **49**, 4023–4045, <https://doi.org/10.1007/s00382-017-3558-4>.
- Back, L. E., and C. S. Bretherton, 2009: On the relationship between SST gradients, boundary layer winds, and convergence over the tropical oceans. *J. Climate*, **22**, 4182–4196, <https://doi.org/10.1175/2009JCLI2392.1>.
- Bechtold, P., M. Köhler, T. Jung, F. Doblas-Reyes, M. Leutbecher, M. J. Rodwell, F. Vitart, and G. Balsamo, 2008: Advances in simulating atmospheric variability with the ECMWF model: From synoptic to decadal time-scales. *Quart. J. Roy. Meteor. Soc.*, **134**, 1337–1351, <https://doi.org/10.1002/qj.289>.
- Brunet, G., and Coauthors, 2010: Collaboration of the weather and climate communities to advance subseasonal-to-seasonal prediction. *Bull. Amer. Meteor. Soc.*, **91**, 1397–1406, <https://doi.org/10.1175/2010BAMS3013.1>.
- Buizza, R., 1997: Potential forecast skill of ensemble prediction and spread and skill distributions of the ECMWF Ensemble Prediction System. *Mon. Wea. Rev.*, **125**, 99–119, [https://doi.org/10.1175/1520-0493\(1997\)125<0099:PFSEOP>2.0.CO;2](https://doi.org/10.1175/1520-0493(1997)125<0099:PFSEOP>2.0.CO;2).
- Chikamoto, Y., H. Mukougawa, T. Kubota, H. Sato, A. Ito, and S. Maeda, 2007: Evidence of growing bred vector associated with the tropical intraseasonal oscillation. *Geophys. Res. Lett.*, **34**, L04806, <https://doi.org/10.1029/2006GL028450>.
- Crueger, T., B. Stevens, and R. Brokopf, 2013: The Madden–Julian oscillation in ECHAM6 and the introduction of an objective MJO metric. *J. Climate*, **26**, 3241–3257, <https://doi.org/10.1175/JCLI-D-12-00413.1>.
- Dee, D. P., and Coauthors, 2011: The ERA-Interim reanalysis: Configuration and performance of the data assimilation system. *Quart. J. Roy. Meteor. Soc.*, **137**, 553–597, <https://doi.org/10.1002/qj.828>.
- DeMott, C. A., N. P. Klingaman, and S. J. Woolnough, 2015: Atmosphere–ocean coupled processes in the Madden–Julian oscillation. *Rev. Geophys.*, **53**, 1099–1154, <https://doi.org/10.1002/2014RG000478>.
- Ferranti, L., T. N. Palmer, F. Molteni, and E. Klinker, 1990: Tropical-extratropical interaction associated with the 30–60 day oscillation and its impact on medium and extended range prediction. *J. Atmos. Sci.*, **47**, 2177–2199, [https://doi.org/10.1175/1520-0469\(1990\)047<2177:TEIAWT>2.0.CO;2](https://doi.org/10.1175/1520-0469(1990)047<2177:TEIAWT>2.0.CO;2).
- Fu, X., B. Wang, D. E. Waliser, and L. Tao, 2007: Impact of atmosphere–ocean coupling on the predictability of monsoon intraseasonal oscillations. *J. Atmos. Sci.*, **64**, 157–174, <https://doi.org/10.1175/JAS3830.1>.
- , —, J. Y. Lee, W. Q. Wang, and L. Gao, 2011: Sensitivity of dynamical intraseasonal prediction skills to different initial conditions. *Mon. Wea. Rev.*, **139**, 2572–2592, <https://doi.org/10.1175/2011MWR3584.1>.
- , J. Y. Lee, P. C. Hsu, H. Taniguchi, B. Wang, W. Wang, and S. Weaver, 2013: Multi-model MJO forecasting during DYNAMO/CINDY period. *Climate Dyn.*, **41**, 1067–1081, <https://doi.org/10.1007/s00382-013-1859-9>.
- , W. Wang, J.-Y. Lee, B. Wang, K. Kikuchi, J. Xu, J. Li, and S. Weaver, 2015: Distinctive roles of air–sea coupling on different MJO events: A new perspective revealed from the DYNAMO/CINDY field campaign. *Mon. Wea. Rev.*, **143**, 794–812, <https://doi.org/10.1175/MWR-D-14-00221.1>.
- Gonzalez, A., and X. Jiang, 2017: Winter mean lower tropospheric moisture over the Maritime Continent as a climate model diagnostic metric for the propagation of the Madden–Julian oscillation. *Geophys. Res. Lett.*, **44**, 2588–2596, <https://doi.org/10.1002/2016GL072430>.
- Gottschalck, J., and Coauthors, 2010: A framework for assessing operational Madden–Julian oscillation forecasts: A CLIVAR MJO Working Group project. *Bull. Amer. Meteor. Soc.*, **91**, 1247–1258, <https://doi.org/10.1175/2010BAMS2816.1>.
- Green, B. W., S. Sun, R. Bleck, S. G. Benjamin, and G. A. Grell, 2017: Evaluation of MJO predictive skill in multiphysics and multimodel global ensembles. *Mon. Wea. Rev.*, **145**, 2555–2574, <https://doi.org/10.1175/MWR-D-16-0419.1>.
- Hagos, S. M., C. Zhang, Z. Feng, C. D. Burleyson, C. De Mott, B. Kerns, J. J. Benedict, and M. N. Martini, 2016: The impact of the diurnal cycle on the propagation of Madden–Julian oscillation convection across the Maritime Continent. *J. Adv. Model. Earth Syst.*, **8**, 1552–1564, <https://doi.org/10.1002/2016MS000725>.
- Ham, Y., S. Schubert, and Y. Chang, 2012: Optimal initial perturbations for ensemble prediction of the Madden–Julian oscillation during boreal winter. *J. Climate*, **25**, 4932–4945, <https://doi.org/10.1175/JCLI-D-11-00344.1>.
- Hamill, T. M., and G. N. Kiladis, 2014: Skill of the MJO and Northern Hemisphere blocking in GEFS medium-range reforecasts. *Mon. Wea. Rev.*, **142**, 868–885, <https://doi.org/10.1175/MWR-D-13-00199.1>.
- Han, J., and H. L. Pan, 2011: Revision of convection and vertical diffusion schemes in the NCEP Global Forecast System. *Weather Forecasting*, **26**, 520–533, <https://doi.org/10.1175/WAF-D-10-05038.1>.
- Hannah, W. M., and E. D. Maloney, 2014: The moist static energy budget in NCAR CAM5 hindcasts during DYNAMO. *J. Adv. Model. Earth Syst.*, **6**, 420–440, <https://doi.org/10.1002/2013MS000272>.
- , —, and M. S. Pritchard, 2015: Consequences of systematic model drift in DYNAMO hindcasts with SP-CAM and CAM5. *J. Adv. Model. Earth Syst.*, **7**, 1051–1074, <https://doi.org/10.1002/2014MS000423>.
- Hendon, H. H., 2000: Impact of air–sea coupling on the Madden–Julian oscillation in a general circulation model. *J. Atmos. Sci.*, **57**, 3939–3952, [https://doi.org/10.1175/1520-0469\(2001\)058<3939:IOASCO>2.0.CO;2](https://doi.org/10.1175/1520-0469(2001)058<3939:IOASCO>2.0.CO;2).
- , and M. L. Salby, 1994: The life cycle of the Madden–Julian oscillation. *J. Atmos. Sci.*, **51**, 2225–2237, [https://doi.org/10.1175/1520-0469\(1994\)051<2225:TLCOTM>2.0.CO;2](https://doi.org/10.1175/1520-0469(1994)051<2225:TLCOTM>2.0.CO;2).
- Hirata, F. E., P. J. Webster, and V. E. Toma, 2013: Distinct manifestations of austral summer tropical intraseasonal oscillations. *Geophys. Res. Lett.*, **40**, 3337–3341, <https://doi.org/10.1002/grl.50632>.
- Hirons, L. C., P. Inness, F. Vitart, and P. Bechtold, 2013a: Understanding advances in the simulation of intraseasonal variability in the ECMWF model. Part I: The representation of the MJO. *Quart. J. Roy. Meteor. Soc.*, **139**, 1417–1426, <https://doi.org/10.1002/qj.2060>.
- , —, —, and —, 2013b: Understanding advances in the simulation of intraseasonal variability in the ECMWF model.

- Part II: The application of process-based diagnostics. *Quart. J. Roy. Meteor. Soc.*, **139**, 1427–1444, <https://doi.org/10.1002/qj.2059>.
- Hsu, P.-C., and T. Li, 2012: Role of the boundary layer moisture asymmetry in causing the eastward propagation of the Madden–Julian oscillation. *J. Climate*, **25**, 4914–4931, <https://doi.org/10.1175/JCLI-D-11-00310.1>.
- Janiga, M. A., and C. Zhang, 2016: MJO moisture budget during DYNAMO in a cloud-resolving model. *J. Atmos. Sci.*, **73**, 2257–2278, <https://doi.org/10.1175/JAS-D-14-0379.1>.
- Jiang, X. D. E., 2017: Key processes for the eastward propagation of the Madden–Julian oscillation based on multimodel simulations. *J. Geophys. Res. Atmos.*, **122**, 755–770, <https://doi.org/10.1002/2016JD025955>.
- , and D. Kim, 2017: Progress and status of MJO simulation in climate models and process-oriented diagnostics. *Sixth Int. Workshop on Monsoons*, Singapore, WMO, 119–124, <https://www.wmo.int/pages/prog/arep/wwrp/new/documents/IWM6AbstractsVolume.pdf>.
- , and Coauthors, 2015: Vertical structure and diabatic processes of the Madden–Julian oscillation: Exploring key model physics in climate simulations. *J. Geophys. Res. Atmos.*, **120**, 4718–4748, <https://doi.org/10.1002/2014JD022375>.
- , Á. F. Adames, M. Zhao, D. E. Waliser, and E. D. Maloney, 2018: A unified moisture mode framework for seasonality of the Madden–Julian oscillation. *J. Climate*, **31**, 4215–4224, <https://doi.org/10.1175/JCLI-D-17-0671.1>.
- Kang, I. S., and H. M. Kim, 2010: Assessment of MJO predictability for boreal winter with various statistical and dynamical models. *J. Climate*, **23**, 2368–2378, <https://doi.org/10.1175/2010JCLI3288.1>.
- , P. H. Jang, and M. Almazroui, 2014: Examination of multi-perturbation methods for ensemble prediction of the MJO during boreal summer. *Climate Dyn.*, **42**, 2627–2637, <https://doi.org/10.1007/s00382-013-1819-4>.
- Kerns, B. W., and S. S. Chen, 2014: Equatorial dry air intrusion and related synoptic variability in MJO initiation during DYNAMO. *Mon. Wea. Rev.*, **142**, 1326–1343, <https://doi.org/10.1175/MWR-D-13-00159.1>.
- , and —, 2016: Large-scale precipitation tracking and the MJO over the Maritime Continent and Indo-Pacific warm pool. *J. Geophys. Res. Atmos.*, **121**, 8755–8776, <https://doi.org/10.1002/2015JD024661>.
- Kiladis, G. N., J. Dias, K. H. Straub, M. C. Wheeler, S. N. Tulich, K. Kikuchi, K. M. Weickmann, and M. J. Ventrice, 2014: A comparison of OLR and circulation-based indices for tracking the MJO. *Mon. Wea. Rev.*, **142**, 1697–1715, <https://doi.org/10.1175/MWR-D-13-00301.1>.
- Kim, D., and E. D. Maloney, 2017: Simulation of the Madden–Julian oscillation using general circulation models. *The Global Monsoon System: Research and Forecast*, C.-P. Chang et al., Eds., World Scientific, 119–130, https://doi.org/10.1142/9789813200913_0009.
- , A. H. Sobel, E. D. Maloney, D. M. W. Frierson, and I. S. Kang, 2011: A systematic relationship between intraseasonal variability and mean state bias in AGCM simulations. *J. Climate*, **24**, 5506–5520, <https://doi.org/10.1175/2011JCLI4177.1>.
- Kim, H. M., 2017: The impact of the mean moisture bias on the key physics of MJO propagation in the ECMWF reforecast. *J. Geophys. Res. Atmos.*, **122**, 7772–7784, <https://doi.org/10.1002/2017JD027005>.
- , and I. S. Kang, 2008: The impact of ocean–atmosphere coupling on the predictability of boreal summer intraseasonal oscillation. *Climate Dyn.*, **31**, 859–870, <https://doi.org/10.1007/s00382-008-0409-3>.
- , P. J. Webster, C. D. Hoyos, and I. S. Kang, 2010: Ocean–atmosphere coupling and the boreal winter MJO. *Climate Dyn.*, **35**, 771–784, <https://doi.org/10.1007/s00382-009-0612-x>.
- , —, V. E. Toma, and D. Kim, 2014: Predictability and prediction skill of the MJO in two operational forecasting systems. *J. Climate*, **27**, 5364–5378, <https://doi.org/10.1175/JCLI-D-13-00480.1>.
- , D. Kim, F. Vitart, V. E. Toma, J. S. Kug, and P. J. Webster, 2016: MJO propagation across the Maritime Continent in the ECMWF Ensemble Prediction System. *J. Climate*, **29**, 3973–3988, <https://doi.org/10.1175/JCLI-D-15-0862.1>.
- Klingaman, N. P., and S. J. Woolnough, 2014: Using a case-study approach to improve the Madden–Julian oscillation in the Hadley Centre model. *Quart. J. Roy. Meteor. Soc.*, **140**, 2491–2505, <https://doi.org/10.1002/qj.2314>.
- , and Coauthors, 2015a: Vertical structure and physical processes of the Madden–Julian oscillation: Linking hindcast fidelity to simulated diabatic heating and moistening. *J. Geophys. Res. Atmos.*, **120**, 4690–4717, <https://doi.org/10.1002/2014JD022374>.
- , X. Jiang, P. K. Xavier, J. Petch, D. Waliser, and S. J. Woolnough, 2015b: Vertical structure and physical processes of the Madden–Julian oscillation: Synthesis and summary. *J. Geophys. Res. Atmos.*, **120**, 4671–4689, <https://doi.org/10.1002/2015JD023196>.
- Lau, K. M., and D. E. Waliser, Eds., 2011: *Intraseasonal Variability in the Atmosphere–Ocean Climate System*. 2nd ed. Springer, 613 pp.
- Lee, J. Y., X. Fu, and B. Wang, 2017: Predictability and prediction of the Madden–Julian oscillation: A review on progress and current status. *The Global Monsoon System: Research and Forecast*, C.-P. Chang et al., Eds., World Scientific, 147–159, https://doi.org/10.1142/9789813200913_0012.
- Lee, S.-S., and B. Wang, 2016: Regional boreal summer intraseasonal oscillation over Indian Ocean and western Pacific: Comparison and predictability study. *Climate Dyn.*, **46**, 2213–2229, <https://doi.org/10.1007/s00382-015-2698-7>.
- , —, D. E. Waliser, J. M. Neena, and J.-Y. Lee, 2015: Predictability and prediction skill of the boreal summer intraseasonal oscillation in the Intraseasonal Variability Hindcast Experiment. *Climate Dyn.*, **45**, 2123–2135, <https://doi.org/10.1007/s00382-014-2461-5>.
- Leutbecher, M., and T. N. Palmer, 2008: Ensemble forecasting. *J. Comput. Phys.*, **227**, 3515–3539, <https://doi.org/10.1016/j.jcp.2007.02.014>.
- , and Coauthors, 2017: Stochastic representations of model uncertainties at ECMWF: State of the art and future vision. *Quart. J. Roy. Meteor. Soc.*, **143**, 2315–2339, <https://doi.org/10.1002/qj.3094>.
- Liebmann, B., and C. A. Smith, 1996: Description of a complete (interpolated) outgoing longwave radiation dataset. *Bull. Amer. Meteor. Soc.*, **77**, 1275–1277, <https://doi.org/10.1175/1520-0477-77.6.1274>.
- Liess, S., D. E. Waliser, and S. D. Schubert, 2005: Predictability studies of the intraseasonal oscillation with the ECHAM5 GCM. *J. Atmos. Sci.*, **62**, 3320–3336, <https://doi.org/10.1175/JAS3542.1>.
- Lim, Y., S. Son, and D. Kim, 2018: MJO prediction skill of the subseasonal-to-seasonal prediction models. *J. Climate*, **31**, 4075–4094, <https://doi.org/10.1175/JCLI-D-17-0545.1>.
- Lin, H., G. Brunet, and J. Derome, 2008: Forecast skill of the Madden–Julian oscillation in two Canadian atmospheric

- models. *Mon. Wea. Rev.*, **136**, 4130–4149, <https://doi.org/10.1175/2008MWR2459.1>.
- Lindzen, R. S. and S. Nigam, 1987: On the role of sea surface temperature gradients in forcing low-level winds and convergence in the tropics. *J. Atmos. Sci.*, **44**, 2418–2436, [https://doi.org/10.1175/1520-0469\(1987\)044<2418:OTROSS>2.0.CO;2](https://doi.org/10.1175/1520-0469(1987)044<2418:OTROSS>2.0.CO;2).
- Ling, J., P. Bauer, P. Bechtold, A. Beljaars, R. Forbes, F. Vitart, M. Ulate, and C. Zhang, 2014: Global versus local MJO forecast skill of the ECMWF model during DYNAMO. *Mon. Wea. Rev.*, **142**, 2228–2247, <https://doi.org/10.1175/MWR-D-13-00292.1>.
- , and Coauthors, 2017: Challenges and opportunities in MJO studies. *Bull. Amer. Meteor. Soc.*, **98**, ES53–ES56, <https://doi.org/10.1175/BAMS-D-16-0283.1>.
- Liu, P., Q. Zhang, C. Zhang, Y. Zhu, M. Khairoutdinov, H. M. Kim, C. Schumacher, and M. Zhang, 2016: A revised real-time multivariate MJO index. *Mon. Wea. Rev.*, **144**, 627–642, <https://doi.org/10.1175/MWR-D-15-0237.1>.
- Liu, X., and Coauthors, 2017: MJO prediction using the sub-seasonal to seasonal forecast model of Beijing Climate Center. *Climate Dyn.*, **48**, 3283–3307, <https://doi.org/10.1007/s00382-016-3264-7>.
- MacLachlan, C., and Coauthors, 2015: Global Seasonal forecast system version 5 (GloSea5): A high-resolution seasonal forecast system. *Quart. J. Roy. Meteor. Soc.*, **141**, 1072–1084, <https://doi.org/10.1002/qj.2396>.
- Madden, R. A., and P. R. Julian, 1971: Detection of a 40–50 day oscillation in the zonal wind in the tropical Pacific. *J. Atmos. Sci.*, **28**, 702–708, [https://doi.org/10.1175/1520-0469\(1971\)028<0702:DOADOI>2.0.CO;2](https://doi.org/10.1175/1520-0469(1971)028<0702:DOADOI>2.0.CO;2).
- , and —, 1972: Description of global-scale circulation cells in the tropics with a 40–50 day period. *J. Atmos. Sci.*, **29**, 1109–1123, [https://doi.org/10.1175/1520-0469\(1972\)029<1109:DOGSCC>2.0.CO;2](https://doi.org/10.1175/1520-0469(1972)029<1109:DOGSCC>2.0.CO;2).
- Maloney, E. D., and A. H. Sobel, 2004: Surface fluxes and ocean coupling in the tropical intraseasonal oscillation. *J. Climate*, **17**, 4368–4386, <https://doi.org/10.1175/JCLI-3212.1>.
- Marshall, A. G., H. H. Hendon, and D. Hudson, 2016: Visualizing and verifying probabilistic forecasts of the Madden–Julian oscillation. *Geophys. Res. Lett.*, **43**, 12 278–12 286, <https://doi.org/10.1002/2016GL071423>.
- , —, S.-W. Son, and Y. Lim, 2017: Impact of the quasi-biennial oscillation on predictability of the Madden–Julian oscillation. *Climate Dyn.*, **49**, 1365–1377, <https://doi.org/10.1007/s00382-016-3392-0>.
- Miyakawa, T., and Coauthors, 2014: Madden–Julian oscillation prediction skill of a new-generation global model demonstrated using a supercomputer. *Nat. Commun.*, **5**, 3769, <https://doi.org/10.1038/ncomms4769>.
- Molteni, F., and T. N. Palmer, 1993: Predictability and finite-time instability of the northern winter circulation. *Quart. J. Roy. Meteor. Soc.*, **119**, 269–298, <https://doi.org/10.1002/qj.49711951004>.
- Moncrieff, M. W., D. E. Waliser, M. J. Miller, M. A. Shapiro, G. R. Asrar, and J. Caughey, 2012: Multiscale convective organization and the YOTC virtual global field campaign. *Bull. Amer. Meteor. Soc.*, **93**, 1171–1187, <https://doi.org/10.1175/BAMS-D-11-00233.1>.
- Moorthi, S., and M. J. Suarez, 1992: Relaxed Arakawa–Schubert: A parameterization of moist convection for general circulation models. *Mon. Wea. Rev.*, **120**, 978–1002, [https://doi.org/10.1175/1520-0493\(1992\)120<0978:RASAP0>2.0.CO;2](https://doi.org/10.1175/1520-0493(1992)120<0978:RASAP0>2.0.CO;2).
- , and —, 1999: Documentation of version 2 of relaxed Arakawa–Schubert cumulus parameterization with convective downdrafts. NOAA Tech. Rep. 99-01, 44 pp.
- Nasuno, T., 2013: Forecast skill of Madden–Julian oscillation events in a global nonhydrostatic model during the CINDY2011/DYNAMO observation period. *Sci. Online Lett. Atmos.*, **9**, 69–73.
- National Academies of Sciences, Engineering, and Medicine, 2016: *Next Generation Earth System Prediction: Strategies for Sub-seasonal to Seasonal Forecasts*. The National Academies Press, 350 pp., <https://doi.org/10.17226/21873>.
- National Research Council, 2010: *Assessment of Intraseasonal to Interannual Prediction and Predictability*. The National Academies Press, 192 pp., <https://doi.org/10.17226/12878>.
- Neena, J. M., J. Y. Lee, D. Waliser, B. Wang, and X. Jiang, 2014: Predictability of the Madden–Julian oscillation in the Intraseasonal Variability Hindcast Experiment (ISVHE). *J. Climate*, **27**, 4531–4543, <https://doi.org/10.1175/JCLI-D-13-00624.1>.
- Nishimoto, E., and S. Yoden, 2017: Influence of the stratospheric quasi-biennial oscillation on the Madden–Julian oscillation during austral summer. *J. Atmos. Sci.*, **74**, 1105–1125, <https://doi.org/10.1175/JAS-D-16-0205.1>.
- Palmer, T. N., Č. Branković, and D. S. Richardson, 2000: A probability and decision-model analysis of PROVOST seasonal multi-model ensemble integrations. *Quart. J. Roy. Meteor. Soc.*, **126**, 2013–2033, <https://doi.org/10.1256/smsqj.56702>.
- , and Coauthors, 2004: Development of a European multi-model ensemble system for seasonal-to-interannual prediction (DEMETER). *Bull. Amer. Meteor. Soc.*, **85**, 853–872, <https://doi.org/10.1175/BAMS-85-6-853>.
- , R. Buizza, F. Doblas-Reyes, T. Jung, M. Leutbecher, G. Shutts, M. Steinheimer, and A. Weisheimer, 2009: Stochastic parametrization and model uncertainty. ECMWF Tech. Memo. 598, 44 pp.
- Pegion, K., and B. P. Kirtman, 2008: The impact of air–sea interactions on the predictability of the tropical intraseasonal oscillation. *J. Climate*, **21**, 5870–5886, <https://doi.org/10.1175/2008JCLI2209.1>.
- Petch, J., D. Waliser, X. Jiang, P. K. Xavier, and S. Woolnough, 2011: A global model intercomparison of the physical processes associated with the Madden–Julian oscillation. *GEWEX News*, No. 3, International GEWEX Project Office, Silver Spring, MD, 3–5.
- Rashid, H. A., H. H. Hendon, M. C. Wheeler, and O. Alves, 2011: Prediction of the Madden–Julian oscillation with the POAMA dynamical prediction system. *Climate Dyn.*, **36**, 649–661, <https://doi.org/10.1007/s00382-010-0754-x>.
- Ray, P., and T. Li, 2013: Relative roles of circumnavigating waves and extratropics on the MJO and its relationship with the mean state. *J. Atmos. Sci.*, **70**, 876–893, <https://doi.org/10.1175/JAS-D-12-0153.1>.
- Raymond, D. J., and Ž. Fuchs, 2009: Moisture modes and the Madden–Julian oscillation. *J. Climate*, **22**, 3031–3046, <https://doi.org/10.1175/2008JCLI2739.1>.
- Reichler, T., and J. O. Roads, 2005: Long-range predictability in the tropics. Part II: 30–60-day variability. *J. Climate*, **18**, 634–650, <https://doi.org/10.1175/JCLI-3295.1>.
- Ren, H. L., and Coauthors, 2017: Prediction of primary climate variability modes at the Beijing Climate Center. *J. Meteor. Res.*, **31**, 204–223, <https://doi.org/10.1007/s13351-017-6097-3>.
- Robertson, A. W., A. Kumar, M. Peña, and F. Vitart, 2015: Improving and promoting subseasonal to seasonal prediction. *Bull. Amer. Meteor. Soc.*, **96**, ES49–ES53, <https://doi.org/10.1175/BAMS-D-14-00139.1>.
- Rui, H., and B. Wang, 1990: Development characteristics and dynamic structure of tropical intraseasonal convection

- anomalies. *J. Atmos. Sci.*, **47**, 357–379, [https://doi.org/10.1175/1520-0469\(1990\)047<0357:DCADSO>2.0.CO;2](https://doi.org/10.1175/1520-0469(1990)047<0357:DCADSO>2.0.CO;2).
- Seo, H., A. C. Subramanian, A. J. Miller, and N. R. Cavanaugh, 2014: Coupled impacts of the diurnal cycle of sea surface temperature on the Madden–Julian oscillation. *J. Climate*, **27**, 8422–8443, <https://doi.org/10.1175/JCLI-D-14-00141.1>.
- Seo, K. H., and W. Wang, 2010: The Madden–Julian oscillation simulated in the NCEP Climate Forecast System model: The importance of stratiform heating. *J. Climate*, **23**, 4770–4793, <https://doi.org/10.1175/2010JCLI2983.1>.
- , —, J. Gottschalck, Q. Zhang, J.-K. Schemm, W. Higgins, and A. Kumar, 2009: Evaluation of MJO forecast skill from several statistical and dynamical forecast models. *J. Climate*, **22**, 2372–2388, <https://doi.org/10.1175/2008JCLI2421.1>.
- Shelly, A., P. Xavier, D. Copey, T. Johns, J. M. Rodriguez, S. Milton, and N. P. Klingaman, 2014: Coupled versus uncoupled hindcast simulations of the Madden–Julian oscillation in the Year of Tropical Convection. *Geophys. Res. Lett.*, **41**, 5670–5677, <https://doi.org/10.1002/2013GL059062>.
- Shukla, J., and Coauthors, 2000: Dynamical seasonal prediction. *Bull. Amer. Meteor. Soc.*, **81**, 2593–2606, [https://doi.org/10.1175/1520-0477\(2000\)081<2593:DSP>2.3.CO;2](https://doi.org/10.1175/1520-0477(2000)081<2593:DSP>2.3.CO;2).
- Sobel, A., and E. Maloney, 2012: An idealized semi-empirical framework for modeling the Madden–Julian oscillation. *J. Atmos. Sci.*, **69**, 1691–1705, <https://doi.org/10.1175/JAS-D-11-0118.1>.
- , and —, 2013: Moisture modes and the eastward propagation of the MJO. *J. Atmos. Sci.*, **70**, 187–192, <https://doi.org/10.1175/JAS-D-12-0189.1>.
- Son, S.-W., Y. Lim, C. Yoo, H. H. Hendon, and J. Kim, 2017: Stratospheric control of the Madden–Julian oscillation. *J. Climate*, **30**, 1909–1922, <https://doi.org/10.1175/JCLI-D-16-0620.1>.
- Straub, K. H., 2013: MJO initiation in the real-time multivariate MJO index. *J. Climate*, **26**, 1130–1151, <https://doi.org/10.1175/JCLI-D-12-00074.1>.
- Subramanian, A. C., and T. Palmer, 2017: Ensemble superparameterization versus stochastic parameterization: A comparison of model uncertainty representation in tropical weather prediction. *J. Adv. Model. Earth Syst.*, **9**, 1231–1250, <https://doi.org/10.1002/2016MS000857>.
- Ventrice, M. J., M. C. Wheeler, H. H. Hendon, C. J. Schreck III, C. D. Thorncroft, and G. N. Kiladis, 2013: A modified multivariate Madden–Julian oscillation index using velocity potential. *Mon. Wea. Rev.*, **141**, 4197–4120, <https://doi.org/10.1175/MWR-D-12-00327.1>.
- Vitart, F., 2014: Evolution of ECMWF sub-seasonal forecast skill scores. *Quart. J. Roy. Meteor. Soc.*, **140**, 1889–1899, <https://doi.org/10.1002/qj.2256>.
- , 2017: Madden–Julian oscillation prediction and teleconnections in the S2S database. *Quart. J. Roy. Meteor. Soc.*, **143**, 2210–2220, <https://doi.org/10.1002/qj.3079>.
- , and T. Jung, 2010: Impact of the Northern Hemisphere extratropics on the skill in predicting the Madden–Julian oscillation. *Geophys. Res. Lett.*, **37**, L23805, <https://doi.org/10.1029/2010GL045465>.
- , and F. Molteni, 2010: Simulation of the Madden–Julian oscillation and its teleconnections in the ECMWF forecast system. *Quart. J. Roy. Meteor. Soc.*, **136**, 842–855, <https://doi.org/10.1002/qj.623>.
- , S. Woolnough, M. A. Balmaseda, and A. Tompkins, 2007: Monthly forecast of the Madden–Julian oscillation using a coupled GCM. *Mon. Wea. Rev.*, **135**, 2700–2715, <https://doi.org/10.1175/MWR3415.1>.
- , and Coauthors, 2017: The Subseasonal to Seasonal (S2S) Prediction project database. *Bull. Amer. Meteor. Soc.*, **98**, 163–173, <https://doi.org/10.1175/BAMS-D-16-0017.1>.
- Waliser, D. E., 2006a: Intraseasonal variability. *The Asian Monsoon*, B. Wang, Ed., Springer, 203–257.
- , 2006b: Predictability of tropical intraseasonal variability. *Predictability of Weather and Climate*, T. Palmer and R. Hagedorn, Eds., Cambridge University Press, 275–305.
- , 2011: Predictability and forecasting. *Intraseasonal Variability of the Atmosphere–Ocean Climate System*, 2nd ed., K. M. Lau and D. E. Waliser, Eds., Springer, 433–476.
- , K. M. Lau, and J.-H. Kim, 1999: The influence of coupled sea surface temperatures on the Madden–Julian oscillation: A model perturbation experiment. *J. Atmos. Sci.*, **56**, 333–358, [https://doi.org/10.1175/1520-0469\(1999\)056<0333:TIOCSS>2.0.CO;2](https://doi.org/10.1175/1520-0469(1999)056<0333:TIOCSS>2.0.CO;2).
- , Z. Zhang, K. M. Lau, and J. H. Kim, 2001: Interannual sea surface temperature variability and the predictability of tropical intraseasonal variability. *J. Atmos. Sci.*, **58**, 2596–2615, [https://doi.org/10.1175/1520-0469\(2001\)058<2596:ISSTVA>2.0.CO;2](https://doi.org/10.1175/1520-0469(2001)058<2596:ISSTVA>2.0.CO;2).
- , K. M. Lau, W. Stern, and C. Jones, 2003: Potential predictability of the Madden–Julian oscillation. *Bull. Amer. Meteor. Soc.*, **84**, 33–50, <https://doi.org/10.1175/BAMS-84-1-33>.
- , and Coauthors, 2006: The Experimental MJO Prediction Project. *Bull. Amer. Meteor. Soc.*, **87**, 425–431, <https://doi.org/10.1175/BAMS-87-4-425>.
- , and Coauthors, 2012: The “Year” of Tropical Convection (May 2008–April 2010): Climate variability and weather highlights. *Bull. Amer. Meteor. Soc.*, **93**, 1189–1218, <https://doi.org/10.1175/2011BAMS3095.1>.
- Wang, W., M. P. Hung, S. J. Weaver, A. Kumar, and X. Fu, 2014: MJO prediction in the NCEP Climate Forecast System version 2. *Climate Dyn.*, **42**, 2509–2520, <https://doi.org/10.1007/s00382-013-1806-9>.
- , A. Kumar, J. X. Fu, and M. Hung, 2015: What is the role of the sea surface temperature uncertainty in the prediction of tropical convection associated with the MJO? *Mon. Wea. Rev.*, **143**, 3156–3175, <https://doi.org/10.1175/MWR-D-14-00385.1>.
- Weisheimer, A., S. Corti, T. Palmer, and F. Vitart, 2014: Addressing model error through atmospheric stochastic physical parametrizations: Impact on the coupled ECMWF seasonal forecasting system. *Philos. Trans. Roy. Soc. London*, **372**, 20130290, <https://doi.org/10.1098/rsta.2013.0290>.
- Wheeler, M. C., and H. H. Hendon, 2004: An all-season real-time multivariate MJO index: Development of an index for monitoring and prediction. *Mon. Wea. Rev.*, **132**, 1917–1932, [https://doi.org/10.1175/1520-0493\(2004\)132<1917:AARMMI>2.0.CO;2](https://doi.org/10.1175/1520-0493(2004)132<1917:AARMMI>2.0.CO;2).
- , H. J. Kim, J. Y. Lee, and J. C. Gottschalck, 2017a: Real-time forecasting of modes of tropical intraseasonal variability: The Madden–Julian and boreal summer intraseasonal oscillations. *The Global Monsoon System: Research and Forecast*, C.-P. Chang et al., Eds., World Scientific, 131–138, https://doi.org/10.1142/9789813200913_0010.
- , H. Zhu, A. H. Sobel, D. Hudson, and F. Vitart, 2017b: Seamless precipitation prediction skill comparison between two global models. *Quart. J. Roy. Meteor. Soc.*, **143**, 374–383, <https://doi.org/10.1002/qj.2928>.
- Woolnough, S. J., F. Vitart, and M. A. Balmaseda, 2007: The role of the ocean in the Madden–Julian oscillation: Implications for MJO prediction. *Quart. J. Roy. Meteor. Soc.*, **133**, 117–128, <https://doi.org/10.1002/qj.4>.

- Wu, J., H.-L. Ren, J. Q. Zuo, C. Zhao, L. Chen, and Q. Li, 2016: MJO prediction skill, predictability, and teleconnection impacts in the Beijing Climate Center atmospheric general circulation model. *Dyn. Atmos. Oceans*, **75**, 78–90, <https://doi.org/10.1016/j.dynatmoce.2016.06.001>.
- Xavier, P. K., and Coauthors, 2015: Vertical structure and physical processes of the Madden–Julian oscillation: Biases and uncertainties at short range. *J. Geophys. Res. Atmos.*, **120**, 4749–4763, <https://doi.org/10.1002/2014JD022718>.
- Xiang, B., M. Zhao, X. Jiang, S. Lin, T. Li, X. Fu, and G. Vecchi, 2015: The 3–4-week MJO prediction skill in a GFDL coupled model. *J. Climate*, **28**, 5351–5364, <https://doi.org/10.1175/JCLI-D-15-0102.1>.
- Yoneyama, K., C. Zhang, and C. N. Long, 2013: Tracking pulses of the Madden–Julian oscillation. *Bull. Amer. Meteor. Soc.*, **94**, 1871–1891, <https://doi.org/10.1175/BAMS-D-12-00157.1>.
- Yoo, C., and S. W. Son, 2016: Modulation of the boreal wintertime Madden–Julian oscillation by the stratospheric quasi-biennial oscillation. *Geophys. Res. Lett.*, **43**, 1392–1398, <https://doi.org/10.1002/2016GL067762>.
- Zhang, C., 2005: Madden–Julian oscillation. *Rev. Geophys.*, **43**, RG2003, <https://doi.org/10.1029/2004RG000158>.
- , 2013: Madden–Julian oscillation: Bridging weather and climate. *Bull. Amer. Meteor. Soc.*, **94**, 1849–1870, <https://doi.org/10.1175/BAMS-D-12-00026.1>.
- , and J. Ling, 2017: Barrier effect of the Indo-Pacific Maritime Continent on the MJO: Perspectives from tracking MJO precipitation. *J. Climate*, **30**, 3439–3459, <https://doi.org/10.1175/JCLI-D-16-0614.1>.
- , J. Gottschalck, E. D. Maloney, M. Moncrieff, F. Vitart, D. E. Waliser, B. Wang, and M. C. Wheeler, 2013: Cracking the MJO nut. *Geophys. Res. Lett.*, **40**, 1223–1230, <https://doi.org/10.1002/grl.50244>.